Magn Reson Med Sci 2022; 21; 9–28
doi:10.2463/mrms.rev.2021-0055 Published Online: August 21, 2021

REVIEW

An Invited Review for the Special 20th Anniversary Issue of MRMS

^{1}H-MR Spectroscopy of the Early Developmental Brain, Neonatal Encephalopathies, and Neurometabolic Disorders

Noriko Aida[1,2*]

MRI interpretations of the pediatric brain are often challenging for general radiologists and clinicians because MR signals and morphology are continuously changing in the developing brain. Furthermore, the developing brain reacts differently to injuries, resulting in imaging characteristics that differ from those of the mature brain. Proton magnetic resonance spectroscopy (^{1}H-MRS) is a non-invasive method for assessing neurological abnormalities at the microscopic level and measures *in vivo* brain metabolites using a clinical MR machine. In MR examinations of the pediatric brain, ^{1}H-MRS demonstrates its powerful diagnostic capability when MRI is insufficient for diagnostic features. MRI and ^{1}H-MRS may be complementary tools for diagnosing and monitoring diseases. However, there is currently no consensus on how to include ^{1}H-MRS in clinical MR examinations. An overview of the clinical implementation of ^{1}H-MRS for the assessment of early pediatric developmental brains as well as the diagnosis, prognostification, and disease monitoring of various non-neoplastic brain disorders, including neonatal encephalopathies and neurometabolic/neurodegenerative diseases, was provided herein. Qualitative and quantitative ^{1}H-MRS is a powerful non-invasive tool for accessing various brain metabolites to confirm age appropriate peaks and detect abnormal peaks or deficient or reduced peaks, which may facilitate the identification of metabolic and neurodegenerative disorders as well as damage associated with hypoxic-ischemic encephalopathy (HIE). Moreover, ^{1}H-MRS has potential as a biomarker for monitoring therapeutic efficacy in metabolic diseases and neonatal HIE. It also provides insights into the pathophysiologies of various disorders, which may facilitate the use of novel therapeutic approaches. Therefore, ^{1}H-MRS needs to be included more frequently in routine clinical MR examinations of pediatric patients with neurological disorders.

Keywords: *magnetic resonance spectroscopy, developmental brain, neonatal encephalopathy, inborn errors of metabolism, neurodegenerative disorder*

Introduction

MRI is the modality of choice for evaluations of central nervous system (CNS) disorders because of its excellent soft tissue contrast. Its imaging capability of morphological details and sensitivity to changes in the content and physical properties of water are high.[1] However, MRI interpretations and precise diagnoses of pediatric brain disorders are often difficult because MR signals in and the morphology of the developing brain are continuously changing. Furthermore, early developing brains show different reactions to injuries, resulting in imaging characteristics that differ from those of the mature brain.[2,3] Conventional MRI cannot depict changes in cell types or biochemical compositions, whereas magnetic resonance spectroscopy (MRS) has this capability. Moreover, the MRI appearance of lesions with different underlying pathophysiologies is often similar. Therefore, MRI and MRS are complementary tools for diagnosing disease and monitoring disease progression and responses to therapy.[1]

Proton magnetic resonance spectroscopy (^{1}H-MRS) is a non-invasive method for assessing neurological abnormalities at the microscopic level and measures *in vivo* brain metabolites using a clinical MR machine.[3] ^{1}H-MRS is frequently employed in evaluations of brain tumors and metabolic disorders not only in adults, but also in children. We

[1]Department of Radiology, Kanagawa Children's Medical Center, Yokohama, Kanagawa, Japan
[2]Department of Diagnostic Radiology, Yokohama City University Graduate School of Medicine, Yokohama, Kanagawa, Japan
*Corresponding author: Department of Radiology, Kanagawa Children's Medical Center, 2-138-4, Mutsukawa, Minami-ku, Yokohama, Kanagawa 232-0066, Japan. Phone: +81457112351, E-mail: naida@kcmc.jp

Received: April 17, 2021 | Accepted: June 5, 2021

more frequently encounter disorders caused by inborn errors of metabolism in the pediatric population than in adults. Under these clinical conditions, ^{1}H-MRS demonstrates its powerful diagnostic capability when MRI is insufficient for diagnostic features. However, there is currently no consensus on how to include ^{1}H-MRS in clinical MR examinations.[4,5] Therefore, an overview of the clinical implementation of ^{1}H-MRS for the assessment of early pediatric developmental brains, as well as the diagnosis, prognostification, and disease monitoring of various non-neoplastic brain disorders, including neonatal encephalopathies and neurometabolic/neurodegenerative disorders, was provided herein, and the clinical impacts and contributions of ^{1}H-MRS were examined.

This review is based on our clinical ^{1}H-MRS database since 2008, which comprises data from more than 5000 pediatric patients (many have more than one study), and the Institute Review Board approved volunteer ^{1}H-MRS studies at Kanagawa Children's Medical Center.

Technical Background of ^{1}H-MRS and Methods

The general technical background of ^{1}H-MRS is described in another special article in this volume by Tomiyasu and Harada.[6]

The major singlet resonance peaks originating from ^{1}H-MRS are as follows: visible N-acetyl aspartate (NAA) or tNAA (i.e., NAA + *N*-acetylaspartylglutamate), creatine (Cr) or tCr (i.e., Cr + phosphocreatine), and choline (Cho) or tCho (i.e., primarily phosphocholine + glycerophosphocholine), which may be quantified at TE up to 280 msec. In short TE MRS, myo-inositol (mIns) and combined glutamate (Glu) and glutamine (Gln) (Glx) may be quantified at 1.5 T, while additional metabolites (e.g., g-aminobutyric acid [GABA] and glutathione) and the separation of Glu and Gln may be quantified at 3.0 T.[1] The main MRS peaks and their significance are as follows: NAA, a neuronal metabolite and *in vivo* biomarker of the presence of viable neurons or the assessment of parenchymal damage, is identified as a resonance peak at 2.0 ppm; Cr, a marker of the energetic reserve, as a peak at 3.0; Cho, a marker of cellular proliferation from increased membrane turnover and/or inflammation, as a peak at 3.2; mIns, a glial metabolite and marker of gliosis, as a peak at 3.5.[1,7] Elevated lactate (Lac), as a doublet peak at 1.3 ppm, reflects anaerobic glycolysis and is a non-specific biomarker of several pathologies.[1] The so-called lipid/macromolecule's peaks at 0.9 and 1.3 ppm are originated from methyl (-CH3) and methylene (-CH2-) groups, respectively. In short TE MRS, small lipid/macromolecule's peaks are seen even in normal cases and increase in cases, such as destructive changes and neoplastic diseases.[8] They overlap Lac peak, which has a sharp doublet peak at 1.3 ppm, but they have broad hems and disappear in long TE MRS.

Since the single-voxel technique is the standard approach used for small volumes, such as deep gray matter (DGM), white matter, and other ROIs, and short TE MRS (TE = 20–35 ms) is sensitive to minor metabolites at low concentrations,[1,9–11] we routinely perform single-voxel short TE MRS as described below. Even in neonates with encephalopathy, we mainly use the same short TE MRS technique instead of long TE MRS (TE = 272–288 ms), which is useful for eliminating baseline noise and assessing the relative concentrations of major peaks and is suitable for hypoxic–ischemic encephalopathy, so as not to overlook underlying metabolic disorders.

^{1}H-MRS data were acquired on 1.5 T and 3.0 T clinical scanners (Magnetom Avanto, Aera, Verio, and Skyla^{fit}; Siemens Healthcare, Erlangen, Germany) between 2008 and 2020. All clinical ^{1}H-MRS data were included in routine brain MR examinations of patients from the Departments of Neurology and Neonatology. Single voxel ^{1}H-MRS was routinely obtained using a point-resolved spectroscopic localization sequence with water presaturation, a TE/TR 30/5000 ms, excitation 8–16, and maximum volumes of interest (VOI) in DGM as the gray matter region, the centrum semiovale (CS) as the white matter region, and the cerebellum (Fig. 1). We added another VOI when we detected pathological lesions on images. VOI locations were selected using transverse, coronal, and sagittal clinical images. The same VOI spectra without a water presaturation pulse were also obtained and used to correct eddy-current-induced phase shifts and quantify metabolite concentrations. ^{1}H-MRS data processing, including signal quantification, was performed using LCModel (Stephen Provencher, Oakville, Canada).

^{1}H-MRS in the Early Developmental Brain

MR spectra continuously change as the brain matures[3] and markedly differ between premature and term infants (Fig. 2). tNAA concentrations are low in a normal, developing, neonatal brain. Brain tNAA concentrations have been shown to rapidly increase with brain maturation from the neonatal period to adolescence with a peak at approximately 10–15 years of age,[4,5] while mIns, Cho, and taurine concentrations decrease with age (Fig. 3).[3] Taurine is an amino acid that is abundant in breast milk and suggested to have an important role in brain development.[12]

Regarding metabolite changes in premature to term infants, between 30 and 43 weeks of postconceptional age (PCA) using a 3T clinical scanner, Tomiyasu et al. reported increases in Cr, NAA, and Glx concentrations with PCA (Fig. 4).[13] The greatest increase was observed in the concentration of NAA: i.e., a more than two-fold increase was observed in DGM and CS between 30 and 43 weeks of PCA. Cr concentrations also increased with PCA, while Cho concentrations remained unchanged. Regarding mIns, its concentration in DGM decreased with PCA but increased in the cerebellum. The increase observed in the cerebellum may be attributed to the later onset of physiological cerebellar development than in the cerebrum.[13] The concentrations

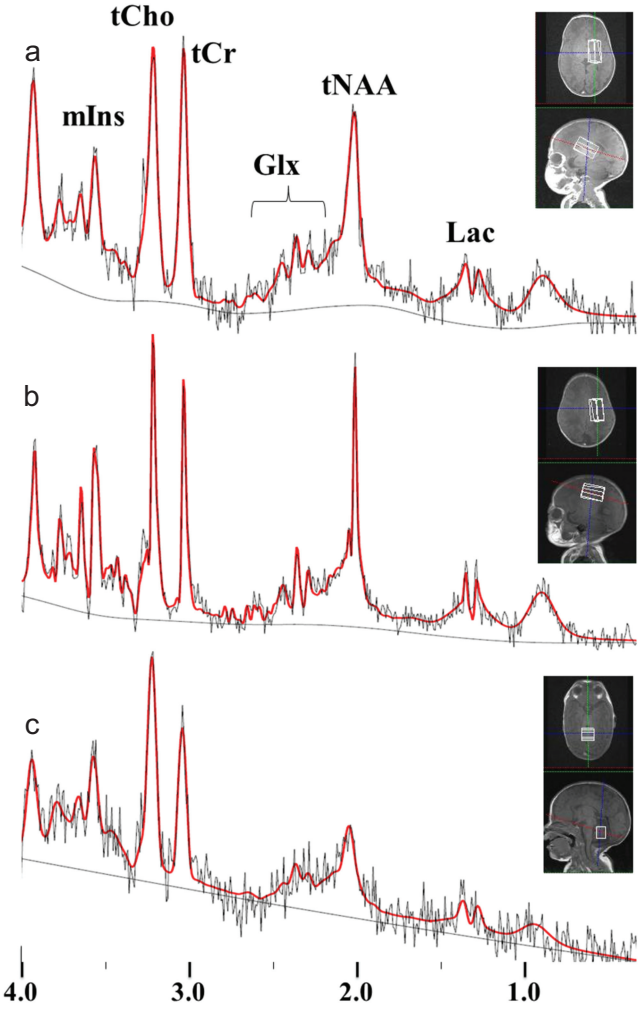

Fig. 1 Representative LCModel outputs of *in vivo* proton Magnetic Resonance spectra for the DGM (**a**), CS (**b**), and cerebellum (**c**); TE/TR, 30/5000 ms) obtained from a neonate. Volumes of interest were imposed on the MR images. In the spectra, the bold red lines represent the fitted lines produced by LCModel, and the thin lines are the original spectra. (Reused from Reference #11). CS, centrum semiovale; DGM, deep gray matter; Glx, glutamate and glutamine; Lac, lactate; mIns, myo-inositol; tCho, glycerophosphocholine (including choline-containing compounds) and phosphocholine; tCr, creatine and phosphocreatine; tNAA, N-acetylaspartate and N-acetylaspartylglutamate.

of all metabolites, except for mIns, were slightly higher in DGM than in CS throughout the neonatal period (Fig. 4).[13] No significant differences were noted in these concentrations between preterm and term infants.[13] These metabolite concentrations and their changes are clinically important as indices of neonatal brain development and may be used as quantified metabolite reference levels in the preterm to term neonatal periods.

Regarding Lac concentrations in the neonatal brain, a previous study reported that preterm and near-term infants with immature metabolic pathways may physiologically undergo anaerobic glycolysis with small Lac peaks.[9] Therefore, the normal range of Lac concentrations and differences between the neonatal brain and that in older children need to be clarified. Using short TE MRS, absolute Lac concentrations in DGM and CS were reported to significantly decrease with age; however, no correlations were detected between either of the regions and PCA during the neonatal period.[14] A more detailed understanding of the normal range of Lac concentrations is important for the precise evaluation of neonatal encephalopathies or other diseases.

Neonatal Encephalopathies

Neonatal encephalopathy is a clinically defined syndrome of impaired neurological function in the earliest days in life; it does not have a specific underlying etiology or pathophysiology, is characterized by consciousness disturbance or seizures, and is often accompanied by difficulties maintaining respiration and the depression of tone and reflexes.[15,16] Various etiologies are associated with neonatal encephalopathies, such as inborn errors of metabolism, intracranial infections, epileptic syndromes, and hypoxic-ischemic events.[15] The condition of a neonate with encephalopathy is critical, and a prompt diagnosis and therapeutic decisions are mandatory to prevent death or permanent long-term neurological sequelae.[17] However, the neurological evaluation of neonates is more difficult than that of older children or adults. MRI and ^{1}H-MRS in the acute phase of neonatal encephalopathies have excellent differential diagnostic abilities. Between 50% and 80% of cases of encephalopathy are considered to have neonatal hypoxic-ischemic encephalopathy (HIE).[15]

Neonatal HIE

Neonatal HIE is a leading cause of mortality and neurological morbidities in children.[17,18] Despite the widespread use of therapeutic hypothermia, approximately 50% of cases still have adverse outcomes.[17] In encephalopathic neonates, the prediction of neurological outcomes is essential for appropriate therapeutic decisions and proper parental counseling for future developmental care. In prognostic assessments, signal changes in DGM on T1 and T2-weighted images (T1WI and T2WI, respectively) are useful after several days to one week.[19,20] Diffusion-weighted images (DWI) are more sensitive for the earlier detection of injured brain parenchyma, generally within a few to several hours.[19,21–23] However, the inspective evaluation of DWI is sometimes confusing mainly because diffusely injured brains are more likely to exhibit widespread signal changes to various degrees, which may lead to the underestimation of less severely injured areas (Fig. 5).[21] Therefore, in the widespread injured brain, an apparent diffusion coefficient (ADC) measurement in each area is necessary for a precise assessment.[21] Nevertheless, the ADC value has a pseudonormalization effect and increases again approximately 5 days after injury.[19,23] Moreover, DWI signal abnormalities change

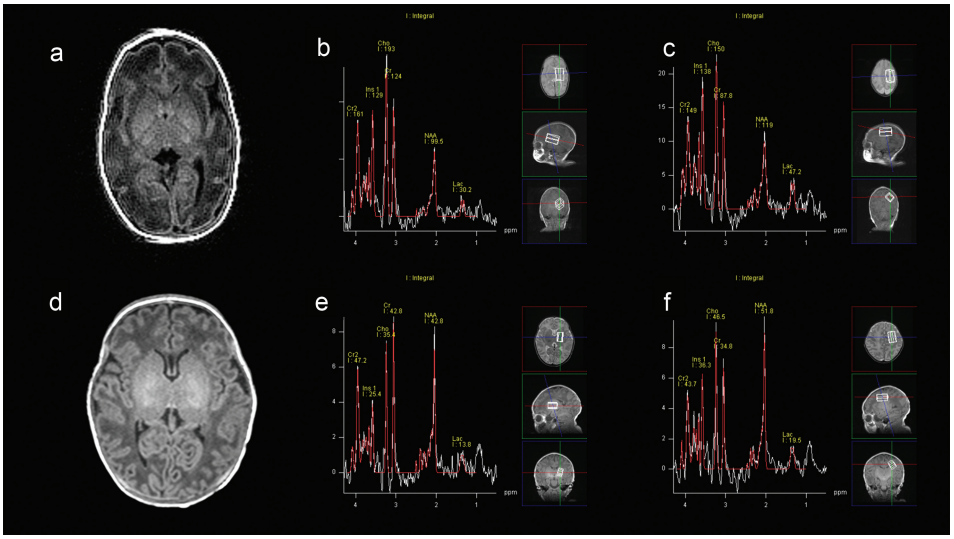

Fig. 2 T1WI and ^{1}H-MRS in the DGM and CS in neonates at PCA of 31 weeks (**a**–**c**) and 40 weeks (**d**–**f**). In a neonate at PCA of 31 weeks (**a**), gyration and sulcation are simpler than those of PCA term neonate (**b**) on MRI. On ^{1}H-MRS, higher Cho and lower NAA are seen at 31 weeks PCA (**b** and **c**) both in DGM and CS compared to those at 40 weeks PCA (**e** and **f**). ^{1}H-MRS, proton magnetic resonance spectroscopy; Cho, choline; CS, centrum semiovale; DGM, deep gray matter; NAA, N-acetyl aspartate; PCA, postconceptional age; T1WI, T1-weighted image.

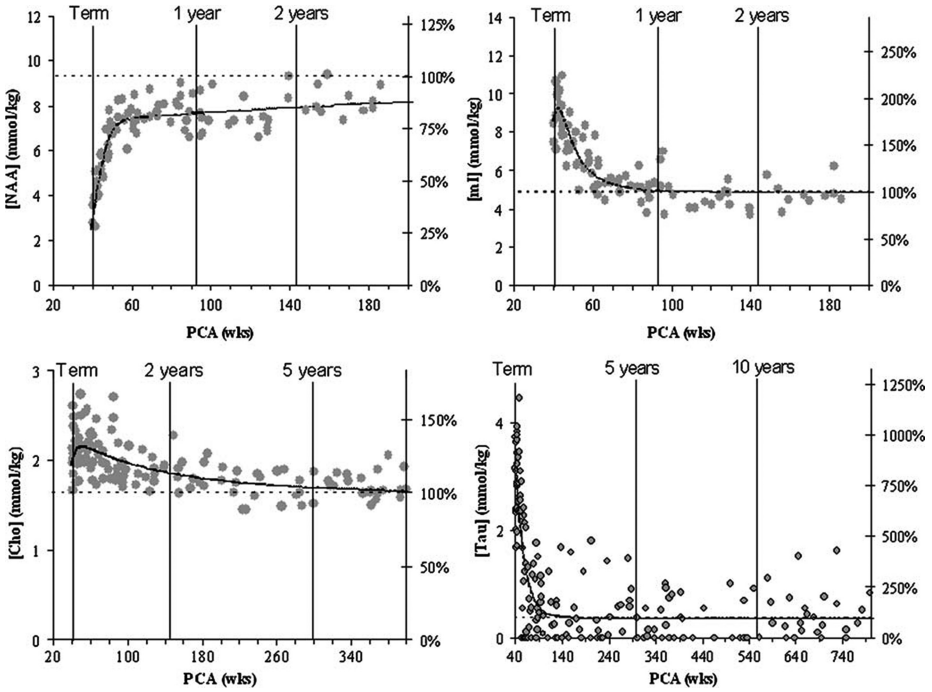

Fig. 3 Quantitation of absolute concentration of metabolites in normal parietal white matter using short TE ^{1}H-MRS. Rapid increase of NAA and decrease in mIns and taurine in particularly at neonate and in infancy are demonstrated. Cho shows gradual decrease. (Reprinted from Reference #3. ^{1}H-MRS, proton magnetic resonance spectroscopy; Cho, choline; mIns, myo-inositol; NAA, N-acetyl aspartate.

daily because fiber-connected areas from the injured parenchyma show high signals due to the so-called remote effects or secondary degeneration (Figs. 5 and 6).[24]

Therefore, a quantitative biomarker is preferable for estimating the degree of injury, which improves neuroprotective assessments and optimizes treatment. Among quantitative markers, ADC values in DGM within 5 days after birth and the brain metabolite ratio, Lac/NAA, measured by ^{1}H-MRS[22,25] have been identified as good neurodevelopmental biomarkers. It is important to note that the evaluation of ADC is limited by its pseudonormalization.[21,26,27] A meta-analysis concluded that the DGM Lac/NAA ratio was the most quantitative biomarker of outcomes.[28] However, since ratios may change with alterations in both denominator and numerator metabolites, the

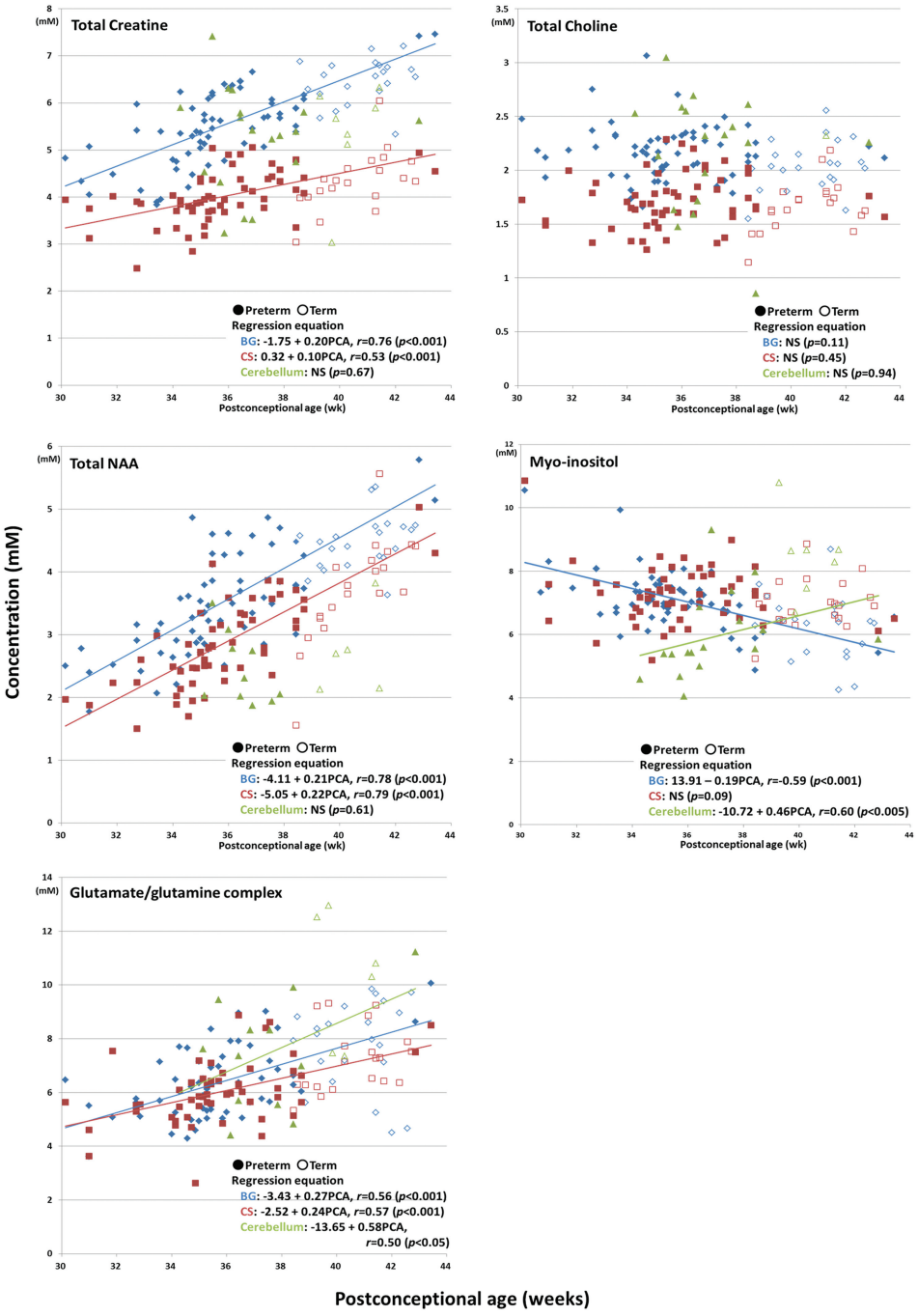

Fig. 4 Scatterplots of the changes in metabolite concentrations with neonatal PCA (weeks); DGM: diamonds, CS: rectangles, and cerebellum: triangles Cr, NAA, and Glx show increases in their concentrations with PCA. NAA demonstrates the greatest elevation. Cho reveals no significant change. Myo-inositol (mIns) concentration decreases with PCA in the DGM, whereas it increases in the cerebellum. In all metabolites except mIns, concentration levels in the DGM tend to be higher than those in the CS. (Reused from Reference #11). Cho, choline; Cr, creatine; CS, centrum semiovale; DGM, deep gray matter; Glx, glutamate and glutamine; NAA, N-acetyl aspartate; PCA, postconceptional age.

underlying pathophysiology remains unclear. Previous studies reported that decreases in the absolute concentrations of NAA and Cho and high Lac concentrations in DGM were associated with poor outcomes in long TE MRS (135–270 msec).[23,25] The evaluation of Glx and mIns concentrations was not possible in long TE MRS. Similarly, the mechanisms underlying changes in metabolite concentrations over time after HIE have not yet been elucidated. With short TE MR spectroscopy, Shibasaki et al. reported time-course changes in the absolute concentrations of NAA, Cho, Cr, Lac, Glx, and mIns and their relationships with neurological outcomes;[29] low absolute concentrations of NAA, Cho, and Cr were identified as accurate prognostic indicators with excellent area under the curve (AUC) values at both 18-96 hours and 7-14 days, and time-dependent reductions in NAA and Cr concentrations predicted adverse outcomes (Table 1).[29] On the other hand, although the prognostic ability of higher Lac and Glx concentrations within 96 hours was also excellent, they were often transient and less

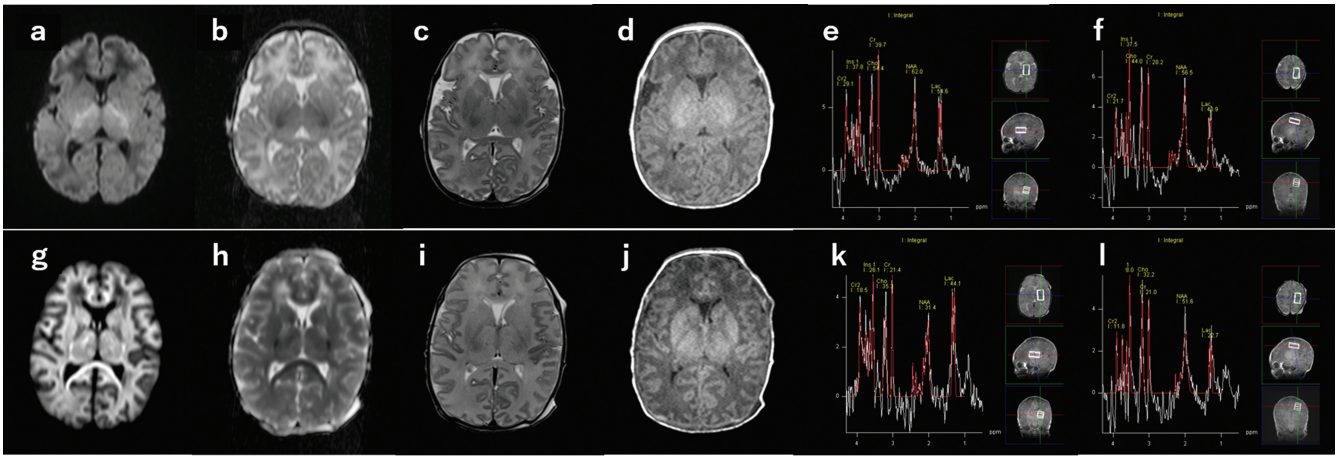

Fig. 5 Evaluation difficulty on early DWI in neonatal HIE. A neonate girl with prolonged profound HIE born at 38 weeks of gestation. DWI (**a**), ADC map (**b**), T2WI (**c**), T1WI (**d**), and ^{1}H-MRS at DGM (**e**) and CS (**f**) at 10 hours after birth. DWI (**g**), ADC map (**h**), T2WI (**i**), T1WI (**j**), and ^{1}H-MRS at DGM (**k**) and CS (**l**) at 3 days. Bilateral posterior internal capsules and part of thalami show symmetrical high signal on DWI with reduced ADC (**a** and **b**) at 10 hours after birth. However, inspective detection of hemispheric abnormalities is difficult on DWI. T1WI and T2WI reveal no detectable abnormality (**c** and **d**). ^{1}H-MRS at DGM (**e**) and CS (**f**) demonstrated prominent Lac peaks. 3 days later, widespread restricted diffusion is apparent both in deep structures and hemispheres (**g** and **h**). T1WI and T2WI demonstrated diffuse high signal in DGM and hemispheric T1, T2 prolongation with swelling (**i** and **j**). ^{1}H-MRSs reveal persistent Lac peaks (**k** and **l**). ^{1}H-MRS, proton magnetic resonance spectroscopy; ADC, apparent diffusion coefficients; CS, centrum semiovale; DGM, deep gray matter; DWI, diffusion weighted images; HIE, hypoxic-ischemic encephalopathy; T1WI, T1-weighted image; T2WI, T2-weighted image.

useful after 7 days (Table 1, Fig. 7).[29] Therefore, caution is needed when using Lac and Glx concentrations more than 7 days after neonatal HIE as predictors. In addition, although previous studies on neonatal HIE did not report time-dependent changes in Glx or mIns concentrations, transiently higher concentrations of Glx followed by decreases in mIns concentrations were observed in neonates with poor outcomes (Table 1, Fig. 7).[29] Furthermore, since NAA, Cr, and Cho concentrations as denominators continued to decrease with time in neonates with poor outcomes, the Lac/NAA, Lac/Cho, and Lac/Cr ratios were naturally of prognostic usefulness with high AUCs (Table 1).[29] These findings suggested the prognostic usefulness of the Lac/NAA, Lac/Cho, and Lac/Cr ratios in daily clinical practice, even without a quantification process. A more detailed understanding of time-course changes in metabolites is important for clarifying the pathophysiology of neonatal HIE.

A multi-center prospective study showed that thalamic NAA concentrations within 14 days after birth were the single best prognostic biomarker with an AUC of 0.99 (95% confidence interval 0.94–1.00) for predicting adverse outcomes 2 years after neonatal HIE. They concluded that ^{1}H-MRS should be a routine component of clinical MR protocols for infants with neonatal HIE, is ideal for early prognostication, and has a potential of a surrogate outcome index.[30]

Neonatal metabolic encephalopathies

Some pediatric patients with inborn errors of metabolism develop a metabolic crisis that manifests as a neonatal encephalopathy. They generally exhibit non-specific symptoms that may mimic more common acute neonatal disorders, such as infections, heart insufficiency, or neonatal HIE, resulting in a possible misdiagnosis. Therefore, neuroimaging is an important diagnostic tool in neonatal metabolic encephalopathies. Although metabolic or genetic laboratory tests are necessary to confirm a diagnosis, MRI may identify an underlying disorder, based on which necessary laboratory investigations will be initiated.[31] Under these conditions, ^{1}H-MRS may contribute to the earlier diagnosis of rare metabolic disorders and facilitate therapeutic decisions and disease monitoring.[31,32]

Two different types of neonatal encephalopathies are described below, and both have a characteristic MR spectrum due to the abnormal accumulation of metabolites:[31] maple syrup urine disease (MSUD) and glycine encephalopathy or nonketotic hyperglycinemia (NKH).

MSUD

MSUD is a rare autosomal recessive inborn error of branched-chain amino acid (BCAA: leucine, valine, and isoleucine) metabolism.[33] In MSUD, infants are normal at birth but rapidly develop encephalopathy from a metabolic crisis before neonatal screening results are obtained.[32] Although an early diagnosis and specific treatment improve outcomes,[34] difficulties are associated with diagnosing MSUD early and several days to weeks are needed to obtain the results of diagnostic examinations in the absence of on-site laboratories. The accumulation of BCAA in the brain is considered to cause myelin instability and vacuolation,

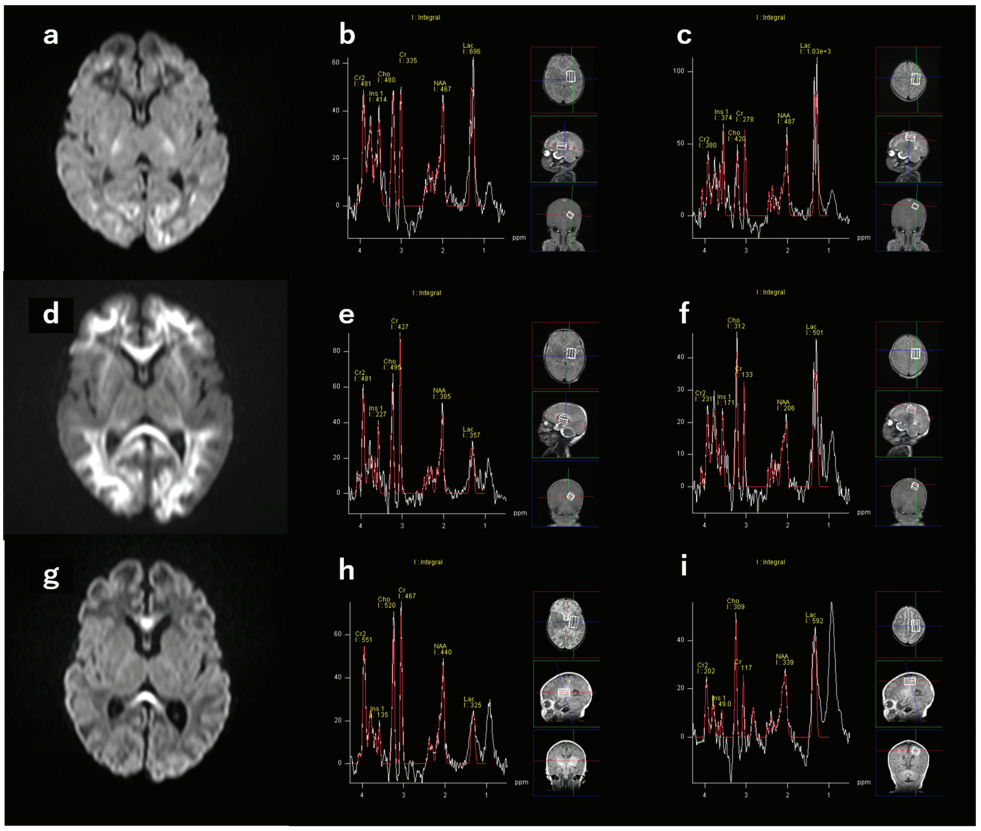

Fig. 6 Dramatical DWI change in neonatal HIE. A neonate boy with prolonged HIE born at 39 weeks of gestation. DWI (**a**, **d**, and **g**) and ^{1}H-MRS at DGM (**b**, **e**, and **h**) and CS (**c**, **f**, and **i**) examined at 7 hours after birth (**a**–**c**), at 4 days (**d**–**f**), and at 11 days (**g**–**i**). Initial MR study reveals restricted diffusion in frontal and occipital cortical/subcortical white matter, as well as in DGM (**a**) with prominent Lac elevation in both DGM and CS (**b** and **c**) on ^{1}H-MRS. At 4 days, widespread diffusion abnormalities are seen in subcortical and deep white matter, and callosum (**d**) with persistent high Lac, reduction in NAA, and elevation in Cho (**e** and **f**). At 11 days, only callosal high signal remains on DWI (**g**) and lipid/macromolecule peaks at 1.3 ppm and 0.9 ppm are apparent (**h** and **i**). ^{1}H-MRS, proton magnetic resonance spectroscopy; Cho, choline; CS, centrum semiovale; DGM, deep gray matter; DWI, diffusion weighted images; HIE, hypoxic-ischemic encephalopathy; NAA, N-acetyl aspartate.

leading to restricted diffusion and T2 prolongation in myelinated tracts;[35] therefore, high intensities are observed in the globus pallidus, thalamus, cerebellar white matter, and dorsal brainstem on DWI and T2WI in encephalopathic neonates with MSUD. However, these findings are not specific. On the other hand, abnormal peaks are detected at approximately 0.9 ppm and 1.3 ppm, overlapping with lipids and Lac peaks, which may also be present.[31] Large peaks at 0.9 have been suggested to originate from BCAA and/or their derivatives, which have more methyl groups (-CH3 at 0.9 ppm) than methylene groups (-CH2- at 1.3 ppm) in MSUD patients;[36] however, the peaks at 0.9 and 1.3 ppm are not specific to MSUD. A large peak at 0.9 ppm, representing the large accumulation of BCAA, may directly provide excessive amounts of leucine, valine, and isoleucine *in vivo* due to an inborn error of BCAA metabolism (Fig. 8). A reduction has been reported in the methyl resonance peak at 0.9 ppm in a neonate with the MSUD metabolic crisis after intensive therapy (Fig. 8).[37] A large methyl resonance peak at 0.9 ppm on brain ^{1}H-MRS may be one of the earliest diagnostic clues of MSUD encephalopathy, based on which physicians may immediately initiate specific intensive therapy.[37]

Glycine encephalopathy (NKH)

Glycine encephalopathy or NKH is an inherited disorder of glycine metabolism that causes the accumulation of high concentrations of glycine in the body, including in the brain, spinal cord, and cerebrospinal fluid (CSF).[38] In neonatal-onset NKH, infants are normal at birth and rapidly manifest lethargy, hypotonia, apnea, and intractable epileptic seizures.[32] On MRI, agenesis/dysgenesis of the corpus callosum is the most common structural abnormality (Fig. 9).[39] On DWI, already myelinated regions at birth are more likely to be primarily involved, similar to MSUD.[32,39] ^{1}H-MRS shows a marked increase of unknown origin overlapping with mIns, which represents glycine (Fig. 9).[32,39,40] However, the signal overlap makes it difficult to differentiate between these two metabolite concentrations, and long TE MRS is helpful because the mIns peak diminishes in the long TE

Table 1 Prognostic use of absolute metabolite concentrations and ratios in deep gray matter for predicting adverse outcomes after neonatal hypoxic-ischemic encephalopathy

(a) Prognostic utility of absolute metabolite concentrations				
Metabolite ratios	Cutoff	Sensitivity (%)	Specificity (%)	AUC
All measurements				
tNAA (mmol/kg wet weight)	4.68	95.5	88.1	0.97 (0.94, 1.00)
tCho (mmol/kg wet weight)	2.24	86.4	85.1	0.94 (0.90, 0.99)
tCr (mmol/kg wet weight)	8.38	81.8	91.0	0.93 (0.88, 0.99)
Lac (mmol/kg wet weight)	1.57	72.7	86.6	0.76 (0.62, 0.91)
Glx (mmol/kg wet weight)	14.79	36.4	95.5	0.61 (0.45, 0.77)
mIns (mmol/kg wet weight)	6.63	50.0	94.0	0.64 (0.45, 0.82)
Measurement at 18–96 h after birth				
tNAA (mmol/kg wet weight)	4.59	100	85.7	0.98 (0.93, 1.00)
tCho (mmol/kg wet weight)	1.95	80.0	93.3	0.94 (0.86, 1.00)
tCr (mmol/kg wet weight)	9.41	100	66.7	0.89 (0.77, 1.00)
Lac (mmol/kg wet weight)	1.62	100	93.3	0.96 (0.88, 1.00)
Glx (mmol/kg wet weight)	13.01	90.0	80.0	0.88 (0.74, 1.00)
mIns (mmol/kg wet weight)	NE	NE	NE	0.37 (0.13, 0.61)
Measurement at 7–14 d after birth				
tNAA (mmol/kg wet weight)	4.68	91.7	88.9	0.97 (0.92, 1.00)
tCho (mmol/kg wet weight)	2.47	100	80.8	0.95 (0.90, 1.00)
tCr (mmol/kg wet weight)	8.38	100	90.4	0.97 (0.94, 1.00)
Lac (mmol/kg wet weight)	1.57	50.0	86.5	0.59 (0.36, 0.82)
Glx (mmol/kg wet weight)	NE	NE	NE	0.36 (0.20, 0.53)
mIns (mmol/kg wet weight)	6.63	91.7	92.3	0.98 (0.94, 1.00)
(b) Prognostic utility of metabolite ratios of metabolites				
Metabolite ratios	Cutoff	Sensitivity (%)	Specificity (%)	AUC
All measurements				
Lac/tNAA	0.443	100	94.0	0.99 (0.97, 1.00)
Lac/tCho	0.387	100	92.5	0.98 (0.96, 1.00)
Lac/tCr	0.475	100	92.5	0.98 (0.97, 1.00)
tNAA/tCr	0.993	95.5	28.4	0.60 (0.46, 0.73)
tCho/tCr	1.333	54.6	77.6	0.67 (0.53, 0.81)
Glx/tCr	NA			
mIns/tCr	0.762	50.0	85.0	0.54 (0.35, 0.73)
Measurement at 18–96 h after birth				
Lac/tNAA	0.443	100	100	1.00 (1.00, 1.00)
Lac/tCho	0.389	100	93.3	0.99 (0.97, 1.00)
Lac/tCre	0.475	100	93.3	0.99 (0.97, 1.00)
tNAA/tCr	1.420	30.0	100	0.58 (0.33, 0.83)

(*Continued*)

Table 1 (Continued).

Metabolite ratios	Cutoff	Sensitivity (%)	Specificity (%)	AUC
tCho/tCr	1.333	50.0	80.0	0.58 (0.33, 0.83)
Glx/tCr	NA			
mIns/tCr	0.770	80.0	80.0	0.82 (0.62, 1.00)
Measurement at 7–14 d after birth				
Lac/tNAA	0.460	100	92.3	0.99 (0.96, 1.00)
Lac/tCho	0.387	100	92.3	0.98 (0.95, 1.00)
Lac/tCre	0.480	100	92.3	0.98 (0.95, 1.00)
tNAA/tCr	0.977	100	28.9	0.58 (0.41, 0.74)
tCho/tCr	1.282	66.7	69.3	0.73 (0.55, 0.90)
Glx/tCr	NA			
mIns/tCr	0.762	25.0	87.1	0.70 (0.46, 0.93)
mIns/tCr	0.762	25.0	87.1	0.70 (0.46, 0.93)

Data are stratified by time of measurement; data in parentheses are 95% confidence intervals. The value of the Glx/tCr ratio was not estimated because it was not displayed on the MR system console. Cutoff values were those with the highest sensitivity and specificity. (Reused from Reference #27). AUC, area under the receiver operating characteristic curve; Glx, glutamate and glutamine; Lac, lactate; mIns, myo-inositol; NA, not available; NE, not estimable; tCho, glycerophosphocholine (including choline-containing compounds) and phosphocholine; tCr, creatine and phosphocreatine; tNAA, *N*-acetylaspartate and *N*-acetylaspartylglutamate.

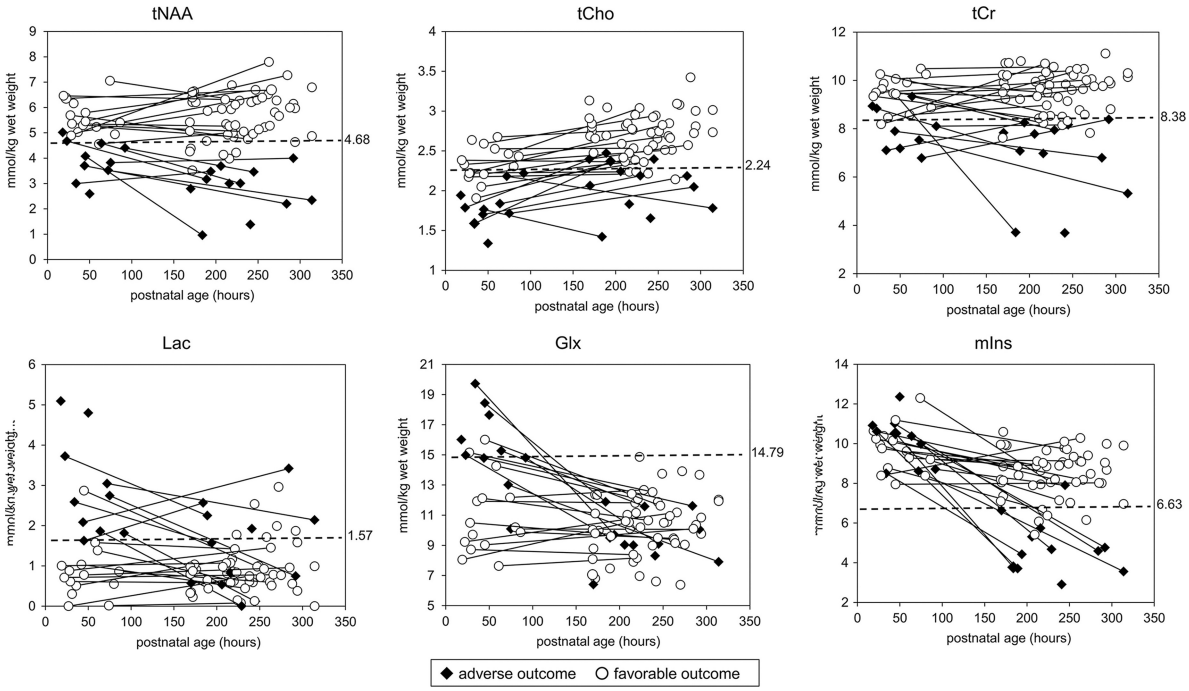

Fig. 7 Time-course changes of absolute concentration of NAA, Cho, Cr, Lac, Glx, and mIns and their relationship with neurological outcome in neonatal HIE. Scatterplots show the distribution of absolute concentrations of six metabolites in the DGM, according to the postnatal age at examination (18–96 hours and 7–14 days after birth). String plots show changes in absolute metabolite concentrations in patients who underwent ^{1}H-MRS at both 18–96 hours and 7–14 days after birth (n = 21). Dotted line indicates the cutoff value for the metabolite obtained by receiver operator characteristic analysis. (Reused from Reference #27). ^{1}H-MRS, proton magnetic resonance spectroscopy; DGM, deep gray matter; Glx, glutamate and glutamine; HIE, hypoxic-ischemic encephalopathy; Lac, lactate; mIns, myo-inositol; tCho, glycerophosphocholine (including choline-containing compounds) and phosphocholine; tCr, creatine and phosphocreatine; tNAA, *N*-acetylaspartate and *N*-acetylaspartylglutamate.

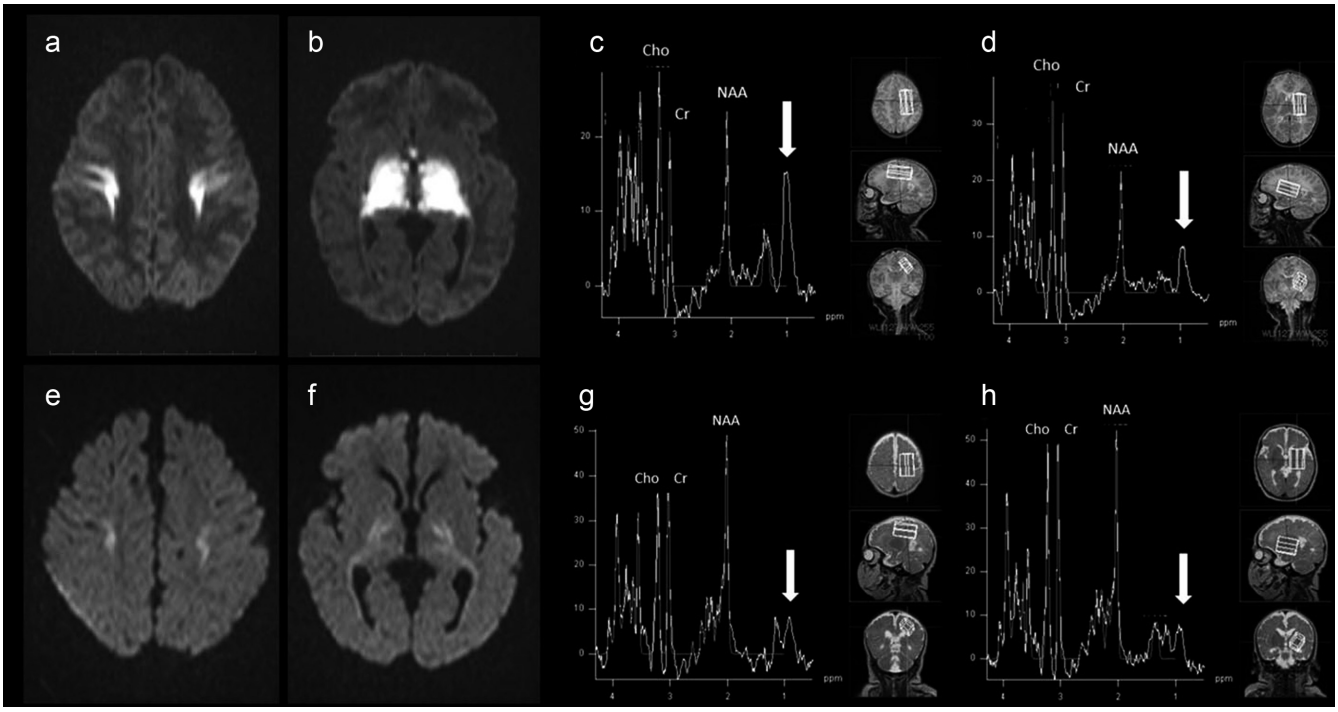

Fig. 8 A neonate boy with encephalopathy from maple syrup urine disease MRI and ^{1}H-MRS findings at (**a**–**d**) onset and in (**e**–**h**) convalescence. Axial DWIs (**a** and **b**) show marked restriction of diffusion in the thalami, the posterior limb of the internal capsule and the globus pallidus. (**c** and **d**) ^{1}H-MRS at the left CS (**c**) and the left DGM (**d**) demonstrate the large peak at 0.9 ppm (arrows) and the decreased NAA peak. Axial DWIs reveal the significant resolution of the hyperintense lesions (**e** and **f**). On ^{1}H-MRS at the left CS (**g**) and DGM (**h**), the decreased peak at 0.9 ppm (arrows) and the increased NAA peak are seen. The Cr level in convalescence was higher than the one at the onset. (Reused from Reference #35). ^{1}H-MRS, proton magnetic resonance spectroscopy; Cho, choline; Cr, creatine; CS, centrum semiovale; DGM, deep gray matter; DWI, diffusion weighted images; NAA, *N*-acetyl aspartate.

sequence.[39] Although the quantification of each metabolite separately is not simple, clinical symptoms and cerebrospinal fluid (CSF) glycine concentrations correlated with glycine + the mIns/Cr ratio, particularly on longer TE ^{1}H-MRS, in a neonate onset NKH patient.[39] Therefore, ^{1}H-MRS indicates a diagnosis of NKH and may be used to monitor the effects of therapeutic interventions, such as the administration of sodium benzoate.[39,40]

Metabolic Emergencies Occurring from the Neonatal Period to Infancy/Childhood

Among inborn errors of metabolism, several disorders may manifest a metabolic crisis either in the neonatal period, infancy, or childhood. Some of these metabolic emergencies with demonstrable radiological and/or ^{1}H-MRS abnormalities are described below.

Organic acid disorders (methylmalonic and propionic acidemia)

Cases of methylmalonic and propionic acidemia often present encephalopathy early in life with episodes of metabolic acidosis, lethargy, vomiting, tachypnea, and seizures sometimes leading to coma. Other cases may present variable symptoms from encephalopathy to learning disabilities or seizures later in life.[41] MRI reveals an abnormal signal change due to increased water content in both myelinated and unmyelinated structures.[3,41] Diffuse swelling may be present on MRI of neonatal onset (Fig. 10).[41] In infancy, methylmalonic acidemia may show a symmetrical change in the globus pallidus, and propionic acidemia in the white matter, putamina, and caudate.[41,42] ^{1}H-MRS is reported to detect reductions in mIns and NAA concentrations.[3] Elevations in Glu and Lac concentrations secondary to hyperammonemia, ketoacidosis, and mitochondrial dysfunction have been reported in patients with a metabolic crisis.[3,31,43] In four neonatal cases of methylmalonic acidemia, all showed white matter edema without restricted diffusion and ^{1}H-MRS revealed low NAA concentrations in both neonates with encephalopathy and those diagnosed in mass screening, and encephalopathic neonates had a high Lac peak (Fig. 10).[43]

Disorders of the urea cycle

Urea cycle defects include ornithine carbamoyl transferase (OTC) deficiency, carbamoyl phosphate synthetase deficiency, argininosuccinic aciduria, citrullinemia, and hyperargininemia, and all result in hyperammonemia.[3] Depending

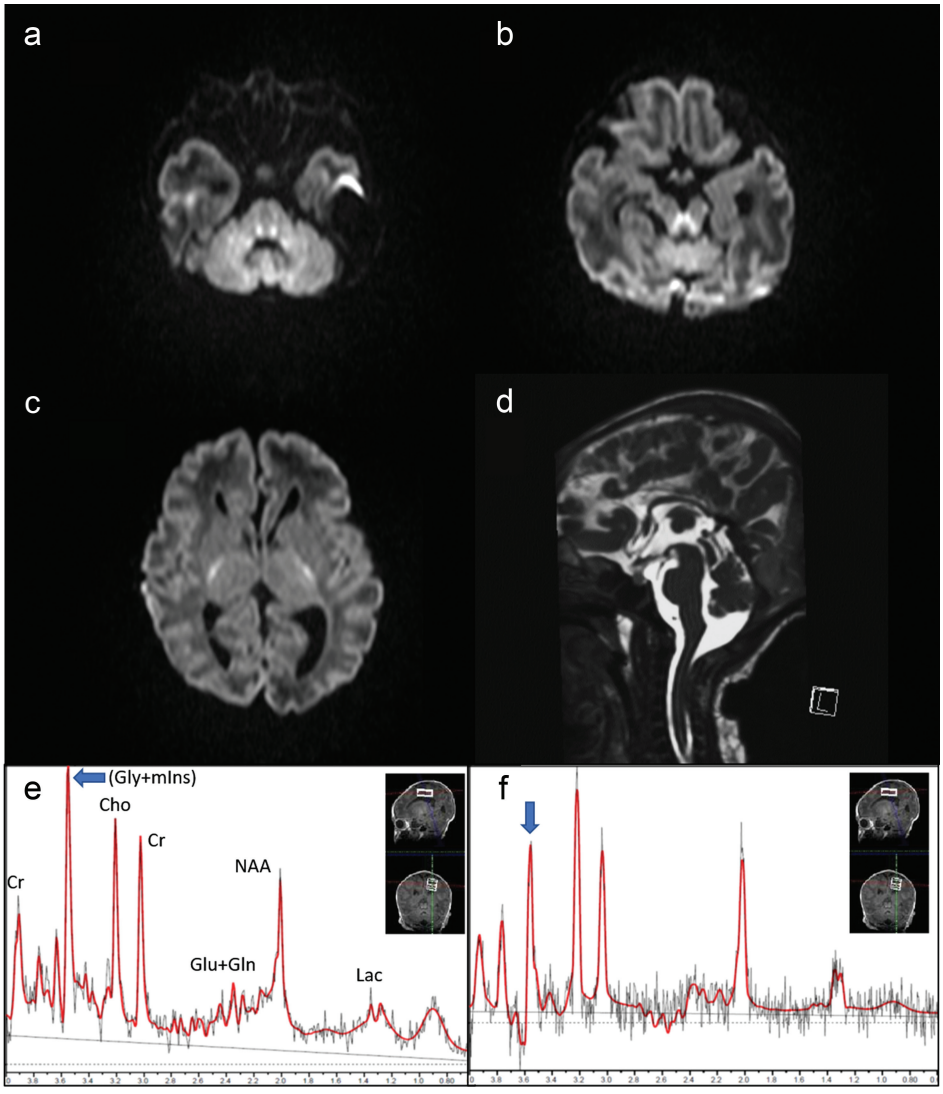

Fig. 9 MRI (**a**-**d**) and LCModel outputs of ^{1}H-MRS (**e**: TE = 30, **f**: TE = 277) in a 6-day-old neonate with glycine encephalopathy DWIs (**a**-**c**) demonstrated symmetrical high signals along the tegmental tracts, superior cerebellar peduncles, and posterior internal capsule. The corpus callosum is small and thin (**d**). Prominent high peaks at 3.55–3.56 ppm representing Gly + mIns, which persists at long TE MRS (TE = 270), are shown (**e** and **f**, arrows). ^{1}H-MRS, proton magnetic resonance spectroscopy; Cho, choline; Cr, creatine; DWI, diffusion weighted images; Gln, Glutamine; Glu, Glutamate; Gly, Glycine; Lac, lactate; mIns, myo-inositol; NAA, *N*-acetyl aspartate.

on the severity of the enzyme deficiency, the onset on the disease varies from soon after birth, in infancy, and to childhood. Ammonia can across the blood-brain barrier and is immediately converted to Gln, which may cause brain edema due to astrocyte swelling.[42] ^{1}H-MRS detects elevations in Gln or Glx concentrations (Fig. 11). Insular and cingulate cortex involvement is often observed on MRI with abnormalities in the perirolandic area and basal ganglia. The so-called scalloped ribbon pattern of injury to the depth of the sulcus in the insular cortex on DWI strongly supports the diagnosis of urea cycle disorders (Fig. 11).[31,42,44,45] In encephalopathic neonates with urea cycle defects, the thalamus is affected less than in those with hypoxic-ischemic insults.[3,31] ^{1}H-MRS detects elevated Gln concentrations on 3.0 T and high Glx concentrations on 1.5 T in short TE, resulting from hyperammonemia and often with elevated Lac concentrations.[31,44,45] These pathological elevations may be reversed with treatment.[3]

Mitochondrial disorders

Defects in intracellular energy metabolism cause mitochondrial disorders.[3] Difficulties are associated with the classification of mitochondrial disorders because our understanding of mitochondrial function or mitochondrial disease remains incomplete.[41] Mitochondrial respiratory chain disorders are the most common cause in childhood. Single or multiple organs (the brain, heart, muscles, kidney, liver, endocrine glands, and bone marrow) may be involved, with muscle and/or brain involvement being the most common.[41] A certain percentage of patients develop acute encephalopathy-like symptoms.

MRI shows various combined CNS signal abnormalities, including symmetrical changes in the basal ganglia, brainstem, cerebellum, optic nerve, and spinal cord, as well as asymmetric and symmetrical signal changes in the cerebral cortex and white matter.[7] Diffuse cerebellar atrophy with or without cerebral atrophy is often detected. However,

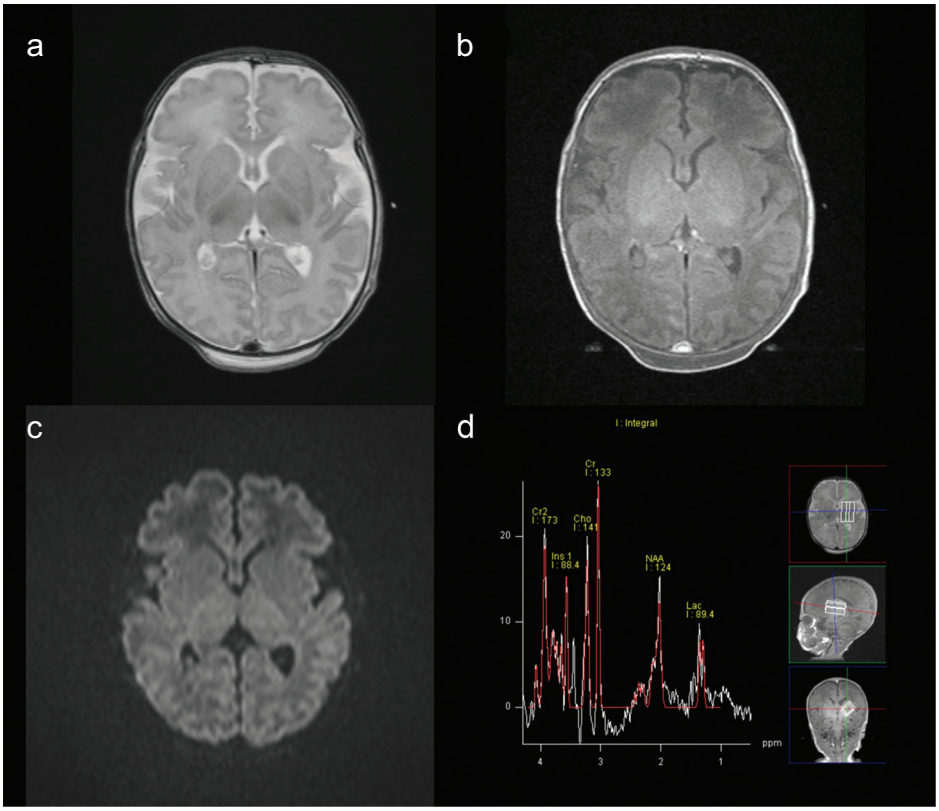

Fig. 10 MRI (**a**-**c**) and ^{1}H-MRS (**d**) in an encephalopathic neonate with Methylmalonic acidemia Diffuse T1 and T2 prolongations in the cerebral white matter are suggested on T1WI (**a**) and T2WI (**b**). No restricted diffusion is seen, but white matter reveals relatively low signal on DWI (**c**). ^{1}H-MRS demonstrates elevated Lac and decreased NAA (**d**). ^{1}H-MRS, proton magnetic resonance spectroscopy; Cho, choline; Cr, creatine; DWI, diffusion weighted images; mIns, myo-inositol; Lac, lactate; NAA, *N*-acetyl aspartate; T1WI, T1-weighted image; T2WI, T2-weighted image.

patients with mitochondrial disease may have a normal brain MRI.[7] Furthermore, the same enzyme or genetic deficiency may show variably different MRI and ^{1}H-MRS patterns, which may be due to the activities of various residual enzymes and complex alternative metabolic pathways.[46] ^{1}H-MRS detects an abnormal high Lac peak within lesions, as well as in normal-appearing parenchyma, reflecting the failure of the respiratory chain with a shift to anaerobic glycolysis. The presence of a small Lac peak in normal-appearing white or gray matter in patients with nonspecific MRI findings suggests an underlying metabolic disease and a subclinical widespread cellular energy failure in mitochondrial disorders.[3,32,46] However, elevated Lac concentrations are not specific for a mitochondrial disorder.[3,41,46] Moreover, it is important to note that the lack of detection of Lac does not exclude the possibility of an underlying mitochondrial disorder.[46] In patients with mitochondrial disorders, NAA concentrations are generally decreased in the areas with elevated Lac concentrations, indicating a neuronal/axonal compromise.[46]

Leigh disease is a multisystem disorder, and the responsible defect may be at nearly every mitochondrial complex level of both mitochondrial and nuclear DNA; however, the majority have mutations in respiratory chain complexes I, IV, and IV and PDHC.[3,41] MRI shows progressive lesions, most frequency in the lentiform nuclei and caudate nuclei; however, signal abnormalities involving the thalamus, periaqueductal gray matter, tegmentum, red nuclei, and dentate nuclei are also common.[46] Although almost no genotype–phenotype correlation exists, *SURF1* (complex IV) mutations may be present in the subthalamic nuclei, medulla, central tegmental tract and reticular formation in the dorsal pons, inferior cerebellar peduncles, cerebellar dentate nuclei, and substantia nigra (Fig. 12).[41,47] DWI and ^{1}H-MRS findings vary depending on the activity of a lesion.[41,47] ^{1}H-MRS shows decreased NAA and elevated Lac concentrations, the latter of which are prominent in acute lesions most severely affected on MRI. However, Lac may be absent at the time of MRI.[41] Therefore,^{1}H-MRS may be a better biomarker for monitoring disease or therapeutic effects than serum Lac concentrations.[46]

Mitochondrial myopathy, encephalopathy, lactic acidosis, and stroke-like episodes (MELAS) is a group of disorders caused by point mutations in mitochondrial DNA, and the 3243(A > G) mutation is the most common.[41,46] Affected patients present with reversible or irreversible stroke-like episodes most commonly in the second decade of life. Although the underlying cause of stroke-like episodes has not yet been clarified, the lesion often crosses vascular boundaries, new lesions may appear in different areas in serial studies, and the size of an abnormal signal area on DWI may increase over weeks. ^{1}H-MRS shows high Lac concentrations in affected areas of the brain (Fig. 13); however, the presence of Lac in areas without signal abnormalities on T2WI or DWI is more

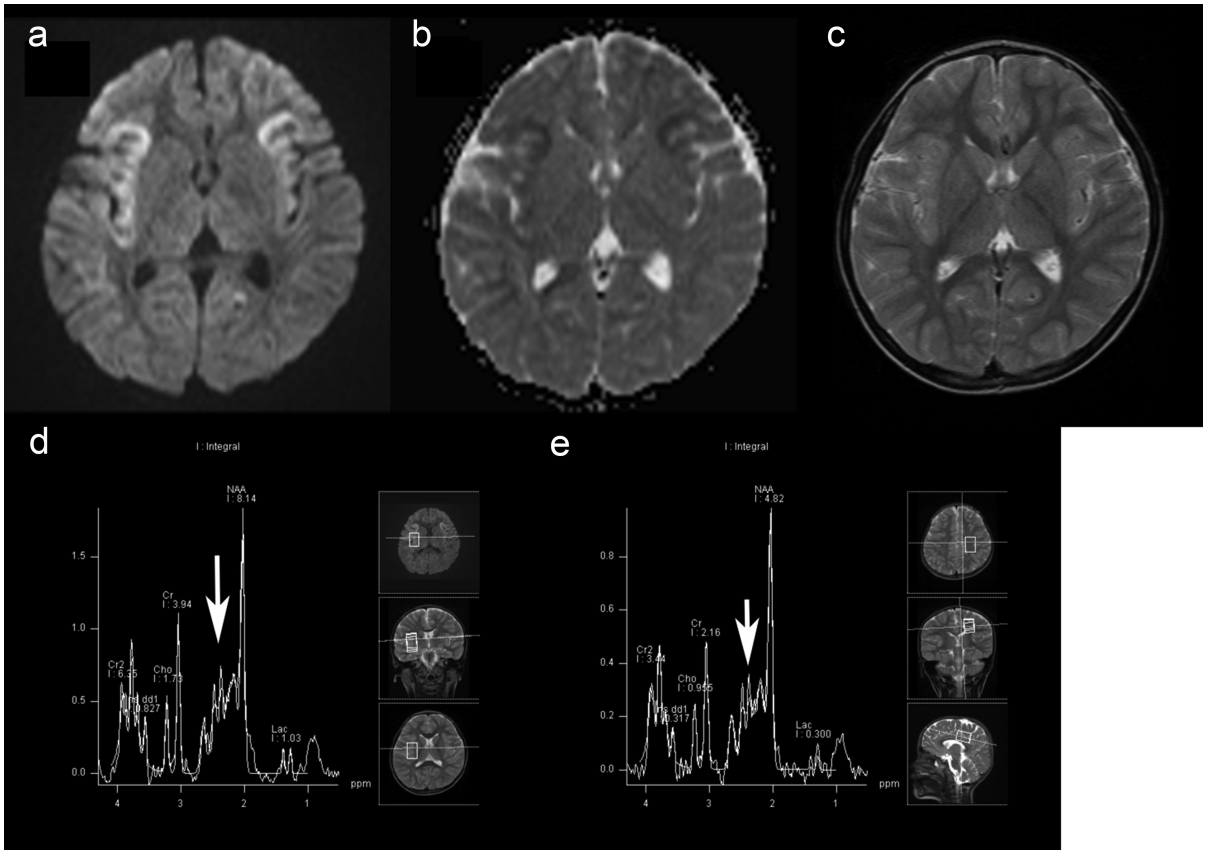

Fig. 11 Scalloped ribbon pattern of injury to the depth of the sulcus in the insular cortex in a 5-year-old boy with OTCD. Symmetrical restricted diffusion of insular cortices is seen (DWI: **a**, ADC map: **b**); however, T2WI reveals normal (**c**). ^{1}H-MRS in the affected insular area (**d**) and Centrum semiovale (**e**) without signal abnormality suggest a slight elevation of Glx (arrows). ^{1}H-MRS, proton magnetic resonance spectroscopy; ADC, apparent diffusion coefficients; Cho, choline; Cr, creatine; DWI, diffusion weighted images; Glx, glutamate and glutamine; mIns, myo-inositol; Lac, lactate; NAA, *N*-acetyl aspartate; OTCD, ornithine carbamoyl transferase deficiency; T2WI, T2-weighted image.

suggestive.[41,46] Even in reversible stroke-like events without DWI or T2WI/fluid-attenuated inversion recovery (FLAIR) signal abnormalities, MRS may show a Lac peak, which matches the neurological symptom (Fig. 13).[48] Perfusion studies and MR arterial spin labeling revealed increased local blood flow in acutely affected areas.[41,49]

GABA metabolism abnormalities

Inborn errors of GABA metabolism, succinic semialdehyde dehydrogenase and GABA-transaminase (GABA-T) deficiencies, are very rare, with the latter presenting with neonatal or early infantile-onset encephalopathy.[50–52] MRI reveals scattered white matter DWI abnormalities without a focal signal change in T1WI or T2WI in the acute phase (Fig. 14)[51] and later general atrophy with dysmyelination.[50,52] Despite the difficulties associated with the initial diagnosis of this rare disease with a non-specific encephalopathic onset, ^{1}H-MRS may facilitate its diagnosis by showing underlying abnormal GABA metabolism.[51] The quantification of GABA is challenging due to its low concentration masked by the larger peaks of Glx, Cr, and NAA.[53] However, combined with the LCModel method, ^{1}H-MRS may facilitate metabolite separation, particularly under pathologically high concentrations (Fig. 14).[51,52] Moreover, a case report of serial ^{1}H-MRS in a patient with GABA-T deficiency suggested that encephalopathic episodes correlated with GABA concentrations in the basal ganglia and concluded that ^{1}H-MRS combined with the LCModel may be clinically applied to measure region-specific GABA concentrations.[52] Therefore, ^{1}H-MRS may be used not only for diagnostic purposes but also to monitor disease or therapeutic effects in GABA metabolism abnormalities.

Neurodegenerative/Neurometabolic Disorders Without Acute Episodes in Infants and Children

Even in infants and children without a neurological emergency, the early diagnosis of neurometabolic and neurodegenerative disorders is important for appropriate treatment, early care planning, and genetic counseling. MRS may be diagnostic if it detects the abnormal presence of or elevations in the accumulation of causative metabolites that are neurotoxic or alter normal

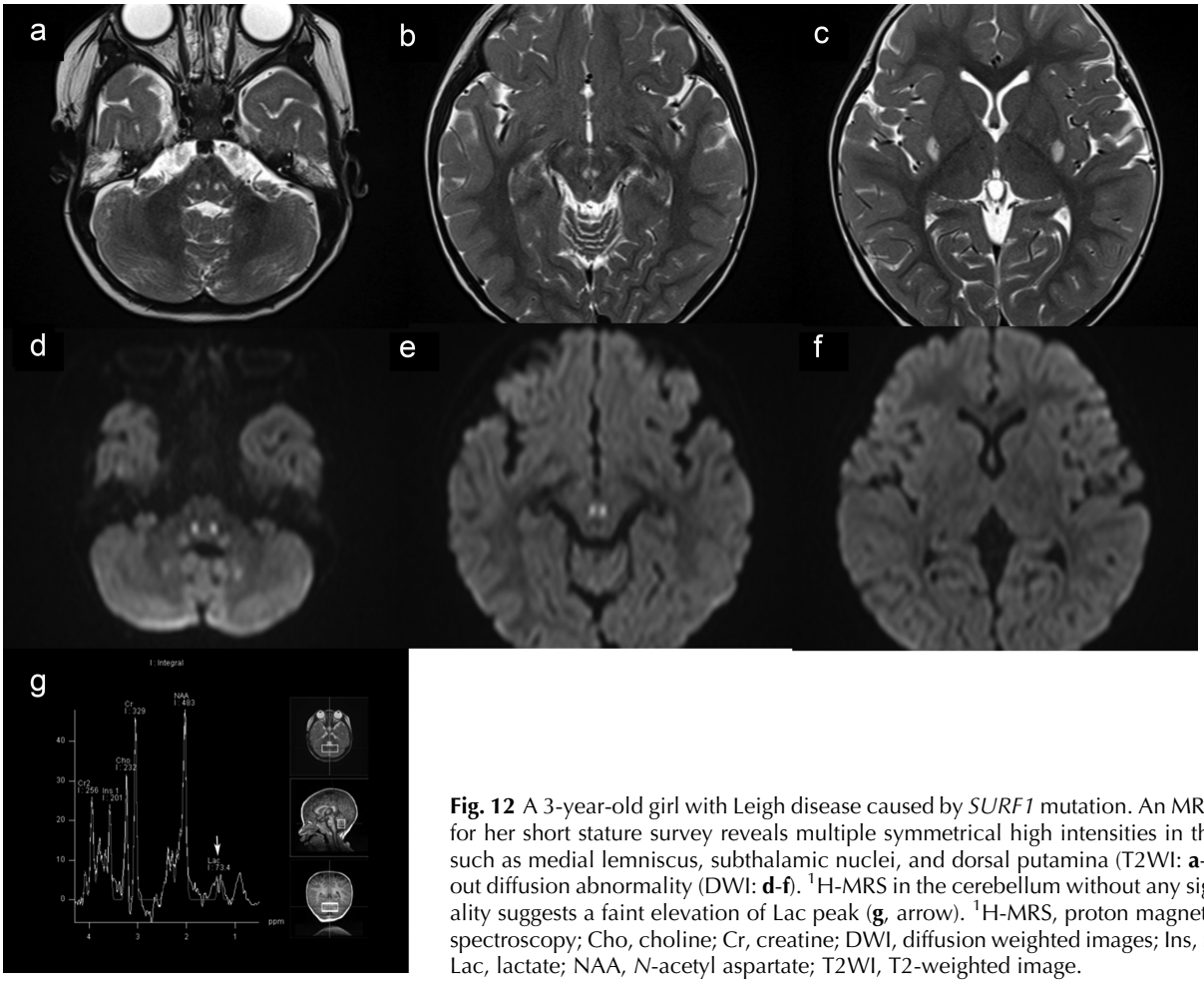

Fig. 12 A 3-year-old girl with Leigh disease caused by *SURF1* mutation. An MR examination for her short stature survey reveals multiple symmetrical high intensities in the brainstem, such as medial lemniscus, subthalamic nuclei, and dorsal putamina (T2WI: **a**-**c**) with/without diffusion abnormality (DWI: **d**-**f**). ^{1}H-MRS in the cerebellum without any signal abnormality suggests a faint elevation of Lac peak (**g**, arrow). ^{1}H-MRS, proton magnetic resonance spectroscopy; Cho, choline; Cr, creatine; DWI, diffusion weighted images; Ins, myo-inositol; Lac, lactate; NAA, *N*-acetyl aspartate; T2WI, T2-weighted image.

function. MRS may also show reductions in metabolites from synthesis or transport abnormalities.[1,31] Some disorders that illustrate these two categories will be described.

Some patients with these disorders present with an uncommon clinical course, as well as almost normal or atypical MRI findings; therefore, a prompt diagnosis at an early stage is often challenging. Under these conditions, ^{1}H-MRS demonstrates its powerful diagnostic capability for detecting an abnormally elevated or deficient/decreased peak.[54,55] Moreover, in neurometabolic/neurodegenerative disorders with a known metabolic causative mechanism and/or therapy, ^{1}H-MRS may be used to monitor the effects of medication or substitution therapy.[31]

Sjögren-Larsson syndrome

Sjögren-Larsson syndrome is characterized by congenital ichthyosis, mental retardation, and spastic paraplegia/tetraplegia. MRI shows delayed myelination in infancy and the subsequent prolongation of T2 in periventricular white matter.[41,56,57] However, the severity of clinical symptoms and white matter abnormalities on MRI varies. ^{1}H-MRS in the white matter shows characteristic narrow peaks at 0.9 and 1.3 ppm (the peak at 1.3 ppm is higher) that are observed even with long TE MRS (Fig. 15), which may be differentiated from broader non-specific macromolecular peaks.[54,56,57] Therefore, in patients without typical clinical or prominent white matter abnormalities, characteristic ^{1}H-MRS findings may facilitate an appropriate molecular survey for a diagnosis.[54]

Cr deficiency syndromes

Cr deficiency is most frequently diagnosed on ^{1}H-MRS as a disorder due to reductions in metabolites caused by synthesis or transport abnormalities.[31] Cr is an essential metabolite for energy storage and transmission in the brain.[32] Three inherited defects in the biosynthesis and transport of Cr have been identified: guanidinoacetate methyltransferase (GAMT) deficiency, L-arginine-glycine amidinotransferase (AGAT) deficiency, and Cr transporter deficiencies caused by the *SLC6A8* mutation at Xq28.[32,41,58] Affected children

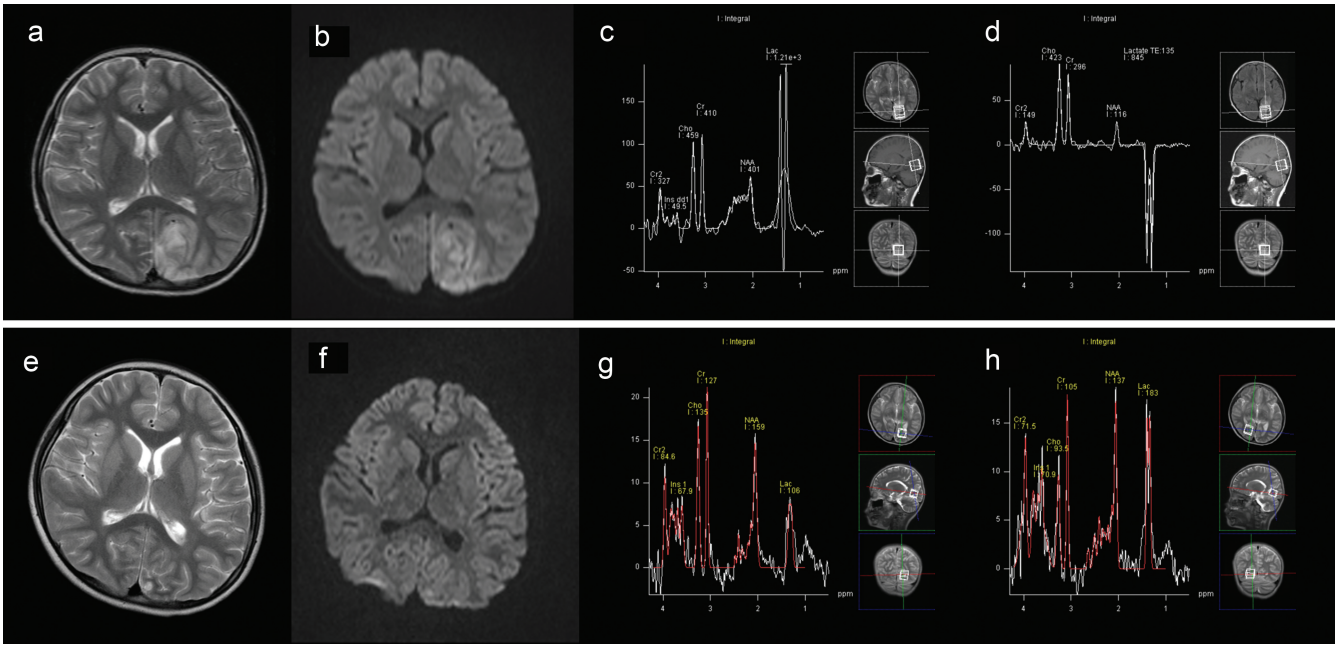

Fig. 13 Sequential brain MRI and ^{1}H-MRS in an 8-year-old girl with MELAS. Axial T2WI (**a**), DWI (**b**), and ^{1}H-MRS in the left occipital lobe (TE = 30: **c**, TE = 135: **d**) at the first stroke-like episode. Axial T2WI (**e**), DWI (**f**), and ^{1}H-MRS in the left (**g**) and right (**h**) occipital lobe at the second stroke-like episode. T2WI (**a**) and DWI (**b**) demonstrate a high-intensity signal in the left occipital region with a prominent doublet peak of lactate (**c** and **d**) at the day of her first classic stroke-like episode. When the girl experienced a second stroke-like episode similar to the first attack 10 d later, MRIs (**e** and **f**) show no abnormal signal in the right occipital region and a residual slightly high-intensity signal in the right occipital region caused by the first episode, whereas ^{1}H-MRS in the right occipital lobe (**h**) demonstrates an elevation of doublet Lac peak, suggesting the underlying mild stroke-like attack. ^{1}H-MRS in the left occipital region (**g**) shows decreased NAA and slightly high but decreased Lac compared to the initial ^{1}H-MRS (**c**), which is consistent with natural time course. (Reused and adopted from Reference #46 and added by the author). ^{1}H-MRS, proton magnetic resonance spectroscopy; Cho, choline; Cr, creatine; DWI, diffusion weighted images; Ins, myo-inositol; Lac, lactate; MELAS, mitochondrial myopathy, encephalopathy, lactic acidosis, and stroke-like episodes; NAA, *N*-acetyl aspartate; T2WI, T2-weighted image.

present with mild-to-moderate developmental delays and severe language impairments. Although MRI is typically almost normal, patients with Cr transporter deficiency show a slightly smaller callosum (Fig. 16).[59] Deficient Cr in cerebral ^{1}H-MRS is a characteristic hallmark[56] as a markedly reduced or completely absent Cr peak at 3.0 ppm (Fig. 16).

Although mutations in *SLC6A8* have been detected in up to 1% of male patients with intellectual disability and/or autistic spectrum disorders,[60–62] it may be less frequent or underestimated in Japan because only eight families had been diagnosed as of 2018.[63] It is important to make an early diagnosis because the clinical symptoms of AGAT and GAMT deficiencies may be partially or completely reversed by dietary Cr supplementation.[42,58,64] Moreover, treatment for the most common form, Cr transporter deficiency, may be available in the near future because cyclocreatine treatment has been reported to improve cognition in mice with this disorder.[65] Therefore, the early diagnosis of all three forms of Cr deficiency syndromes using ^{1}H-MRS is essential; however, only one patient with GAMT deficiency and none with AGAT deficiency have been reported in Japan to date.[63,66]

Folate transport deficiencies

Among cerebral folate deficiencies, folate transport deficiency (Folate receptor alpha defect) due to a mutation in the *FOLR1* gene is a treatable disorder by folate substitution.[31,67] Affected patients develop psychomotor regression, movement disorders, epilepsy, and white matter abnormality in late infancy.[67] Folinic acid is an easily available drug that is often used in combination with methotrexate in chemotherapy and may reverse neurological symptoms and brain MRI abnormalities in patients with folate transport deficiency.[67] ^{1}H-MRS shows reduced Cho and mIns concentrations in white matter, which may be due to the detection of a deficit in glial Cho and mIns concentrations.[67] Reduced Cho concentrations may be attributed to increased consumption as an alternative metabolite related to the pathways of myelination.[32,67] The combination of low Cho and mIns concentrations on ^{1}H-MRS suggest this rare metabolic disorder in infants and children with non-specific neurological manifestations (Fig. 17). Moreover, since ^{1}H-MRS abnormalities regress after therapy (Fig. 17), ^{1}H-MRS may also be used to monitor the effectiveness of treatment.

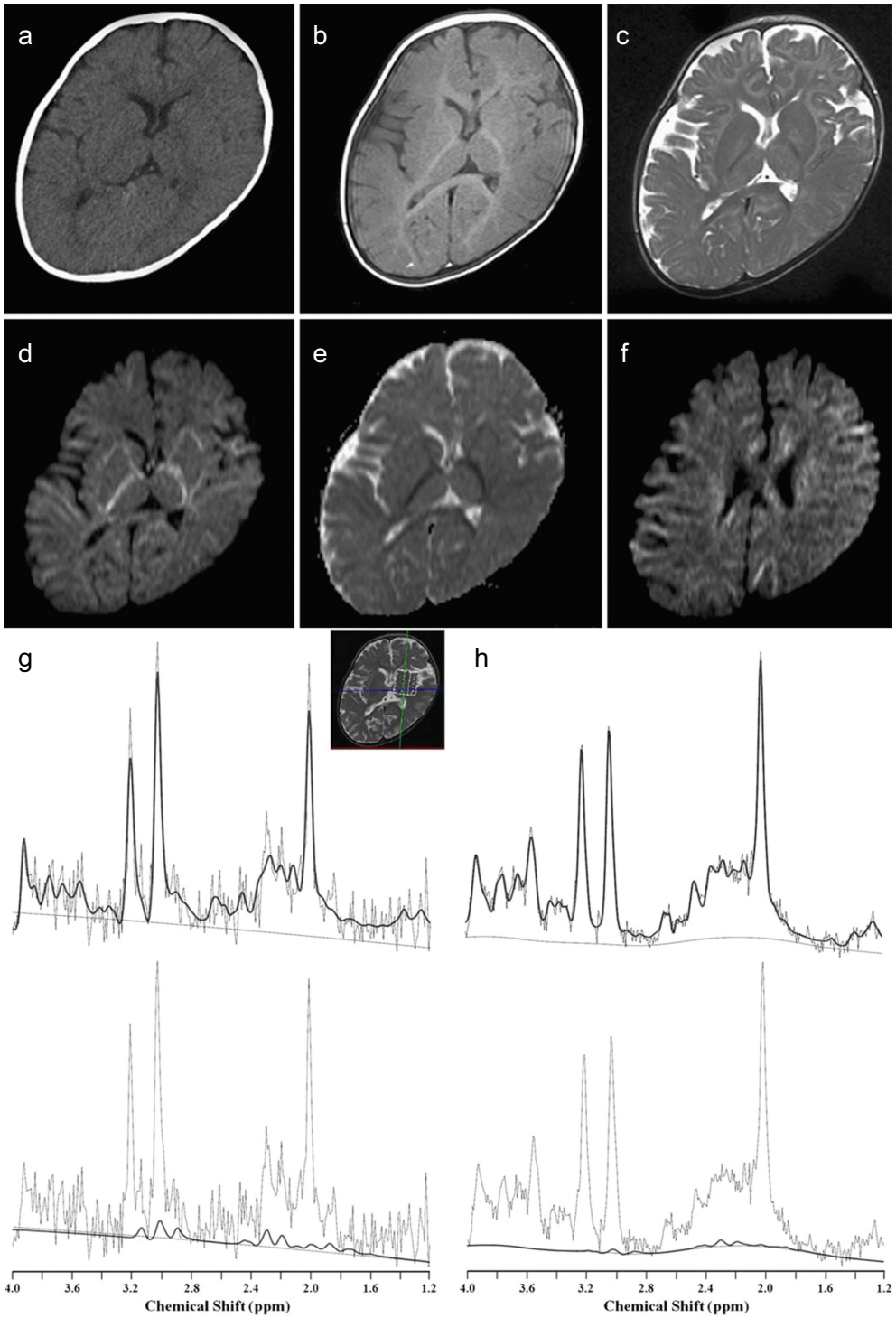

Fig. 14 A 8-month-old girl with GABA-T deficiency CT (**a**), T1WI (**b**), T2WI (**c**), DWI (**d**), and ADC map (**e**) at the level of the basal ganglia, and DWI of the semioval center (**f**). LCModel outputs of ^{1}H-MRS of patient with GABA-T deficiency (8 months) (**g**), and a control individual (7 months) (**h**) from the basal ganglia. CT (**a**) shows no particular abnormality and T1WI (**b**), T2WI (**c**) suggest delayed myelination. DWI (**d** and **f**) shows widespread high signals in the internal and external capsules and many parts of the subcortical white matter, with restricted diffusion (**e**) Bold lines indicate LCModel fitting, and thin lines indicate the original spectra (**g** and **h**). Bold lines in the upper row are the fitting curves of total spectra including all metabolites, and those in the lower row are fitting curves for GABA. The estimated absolute concentrations of GABA in patient and control are 2.9 and 0.8 mmol/l, respectively. Normal GABA spectrum exhibits a quintet ($^{3}CH_2$) at 1.89 ppm, a triplet ($^{4}CH_2$) at 2.28 ppm, and a multiplet resembling a triplet ($^{2}CH_2$) at 3.01 ppm. (Reused from Reference #49). ^{1}H-MRS, proton magnetic resonance spectroscopy; ADC, apparent diffusion coefficients; DWI, diffusion weighted images; GABA-T, gamma aminobutyric acid transaminase; T1WI, T1-weighted image; T2WI, T2-weighted image.

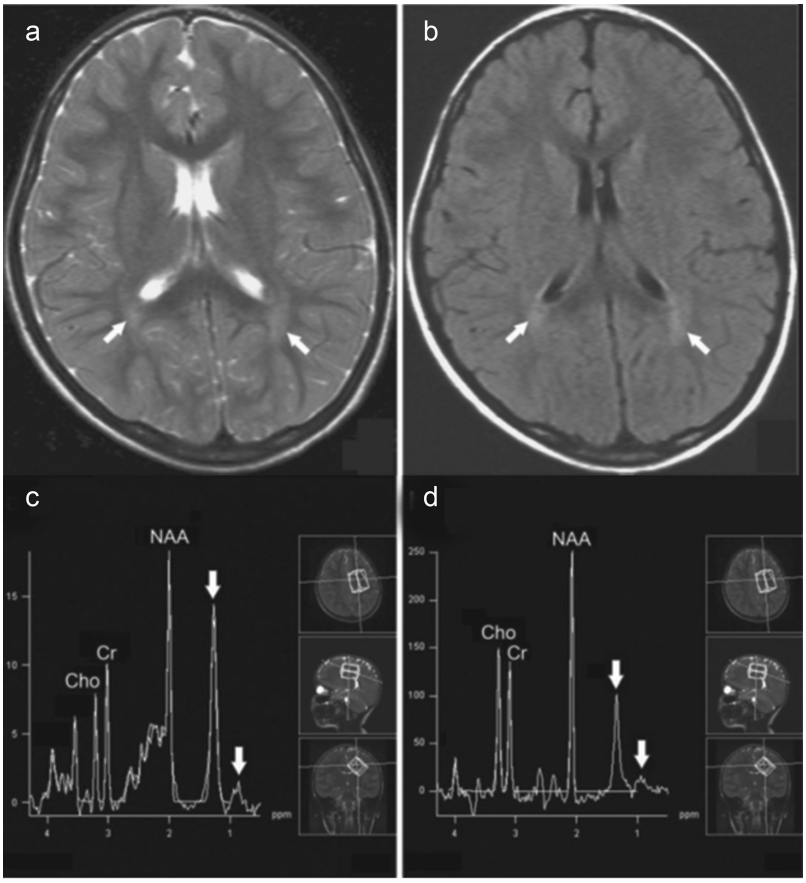

Fig. 15 A 5-year-old girl with Sjögren-Larsson syndrome The minimal high-intensity lesions in the deep white matter around the trigones of the bilateral lateral ventricles on T2WI (**a**) and FLAIR images (**b**) are scarcely distinguishable from a normal nonmyelinated lesion considering her age (arrows). A short (TE = 30, **c**) and long (TE = 135, **d**) TE ^{1}H-MRS at the left centrum-semiovale reveal narrow abnormal resonance peaks at 1.3 ppm and 0.9 ppm (arrows). (Reused from Reference #52). ^{1}H-MRS, proton magnetic resonance spectroscopy; Cho, choline; Cr, creatine; FLAIR, fluid-attenuated inversion recovery; NAA, N-acetylaspartate; T2WI, T2-weighted image.

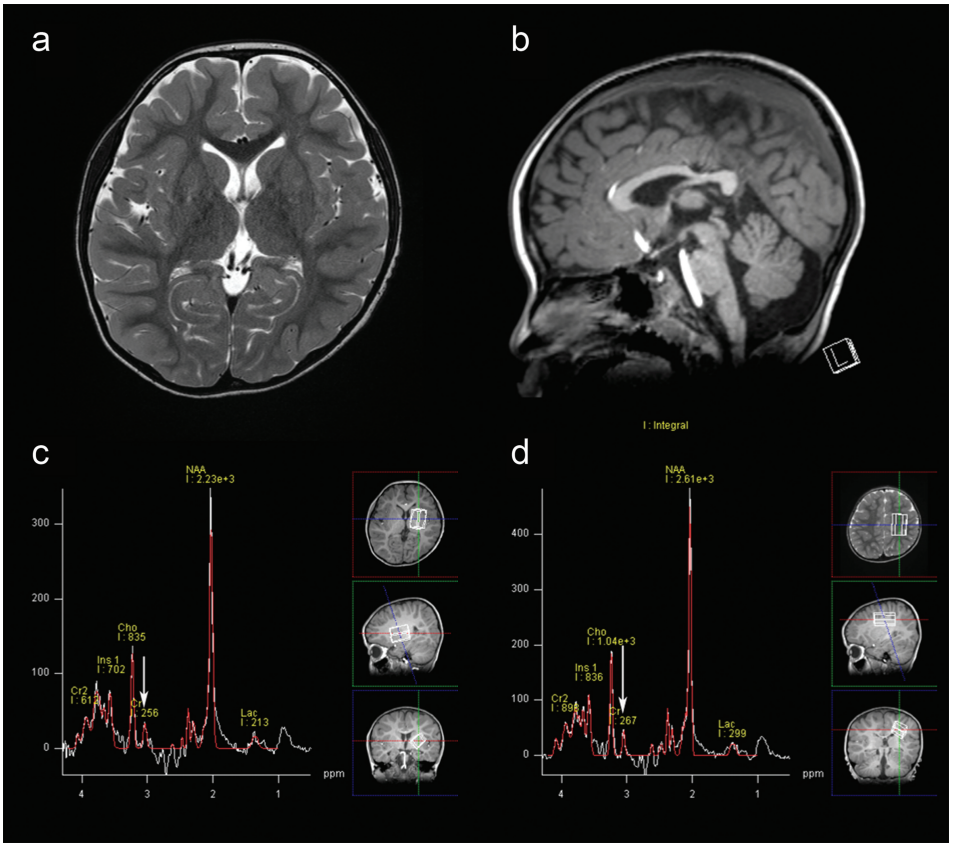

Fig. 16 A 4-year-old boy with Creatine transporter deficiency An axial T2WI (**a**) and a sagittal T1WI (**b**) reveal almost normal other than a little thin callosum. ^{1}H-MRS in DGM (**c**) and CS (**d**) demonstrate deficient Cr peak at 3.0 ppm as pointed arrows. ^{1}H-MRS, proton magnetic resonance spectroscopy; Cho, choline; Cr, creatine; CS, centrum semiovale; DGM, deep gray matter; Ins, myo-inositol; Lac, lactate; NAA, *N*-acetyl aspartate; T1WI, T1-weighted image; T2WI, T2-weighted image.

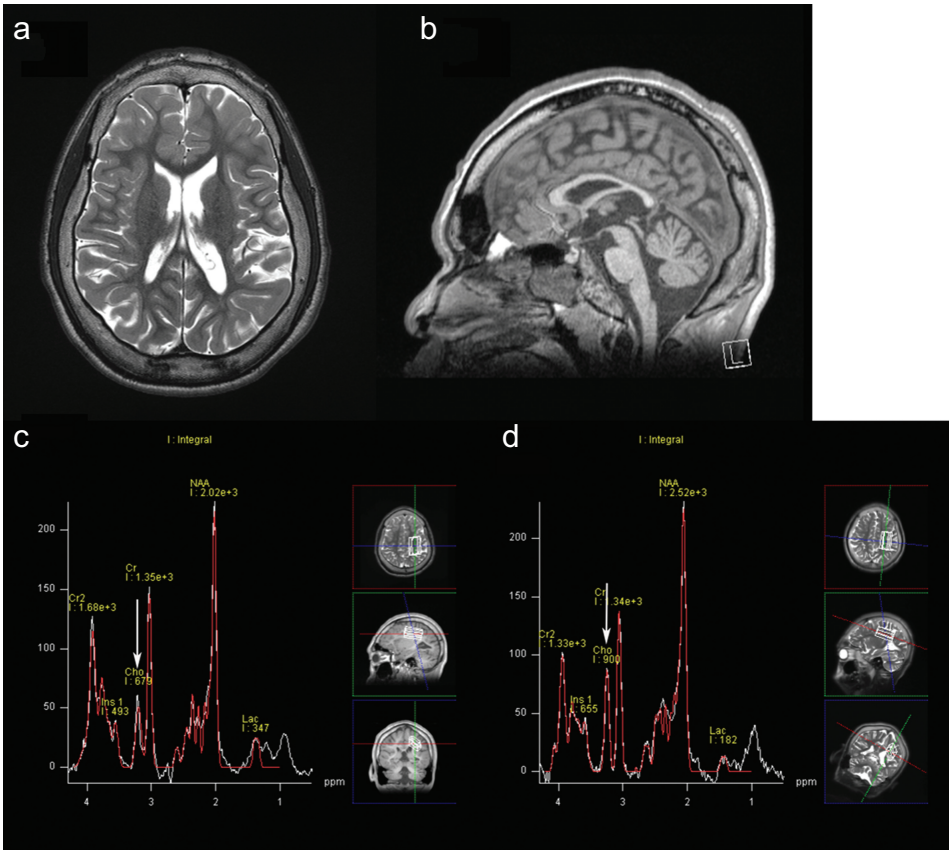

Fig. 17 A 17-year-old boy with folate transport deficiency. An axial T2WI (**a**), sagittal T1WI (**b**), and ^{1}H-MRS in the centrum semiovale before (**c**) and 3 months after (**d**) folinic acid therapy.MRIs show mild brain atrophy and thin callosum. On ^{1}H-MRS, reduced Cho (arrow in **c**) become higher (arrow in **d**) and NAA increases relative to Cr on the study 3 months after folinic acid therapy (**d**). ^{1}H-MRS, proton magnetic resonance spectroscopy; Cho, choline; Cr, creatine; Ins, myo-inositol; Lac, lactate; NAA, *N*-acetyl aspartate; T1WI, T1-weighted image; T2WI, T2-weighted image.

Conclusion

The clinical implementation of ^{1}H-MRS in pediatric CNS disorders is useful for the detection and assessment of the extent of cellular dysfunction. ^{1}H-MRS is sometimes diagnostic for some metabolic disorders but generally demonstrates the degree of a metabolic abnormality.[32] Qualitative and quantitative ^{1}H-MRS is a powerful non-invasive tool for accessing various brain metabolites for the confirmation of age-appropriate peaks, the detection of abnormal peaks, such as glycine and Lac, or the loss of peaks, including Cr[9], which may facilitate the identification of metabolic, neurodegenerative, and destructive disorders in the neonatal period to adolescence. In neonatal HIE, MRS has an immediate impact on therapeutic choices and also helps clinicians with the difficult task of predicting outcomes.[29,30,32] Moreover, ^{1}H-MRS has the potential to serve as a biomarker for monitoring therapeutic efficacy in selected disorders,[9,32] including metabolic diseases and neonatal HIE. Furthermore, ^{1}H-MRS provides a more detailed understanding of the pathophysiology of various disorders, which may facilitate novel therapeutic methods. Therefore, ^{1}H-MRS needs to be included more frequently in routine clinical MR examinations for pediatric patients with neurological disorders.

Funding

The present study was supported by the Japan Society for the Promotion of Science KAKENHI (15K09943, 19K08213, 26461843) and the Kanagawa Municipal Hospital Pediatric Research Fund.

Acknowledgment

The author would like to thank Moyoko Tomiyasu, PhD, for her contribution as a specialist of MRS and the MR technicians at Kanagawa Children's Medical Center for their dedication to pediatric patients.

Conflicts of Interest

The author declares that there are no conflicts of interest.

References

1. Oz G, Alger JR, Barker PB, et al. MRS Consensus Group. Clinical proton MR spectroscopy in central nervous system disorders. Radiology 2014; 270:658–679.
2. Barkovich MJ, Barkovich AJ. Normal Development of the fetal, neonatal, and infant brain, skull, and spine, In:

Barkovich AJ, Rayboud C eds. Pediatric neuroimaging, 6th ed. Philadelphia:Wolters Kluwer, 2019; 18–80.
3. Panigrahy A, Nelson MD Jr, Blüml S. Magnetic resonance spectroscopy in pediatric neuroradiology: clinical and research applications. Pediatr Radiol 2010; 40:3–30.
4. Barta H, Jermendy A, Kolossvary M, et al. Prognostic value of early, conventional proton magnetic resonance spectroscopy in cooled asphyxiated infants. BMC Pediatr 2018; 18:302.
5. Manias KA, Peet A. What is MR spectroscopy? Arch Dis Child Educ Pract Ed 2018; 103:213–216.
6. Tomiyasu M, Harada M. *In vivo* human MR spectroscopy using a clinical scanner: development, applications and future prospects. Magn Reson Med Sci 2022; 21:235–252.
7. Mascalchi M, Montomoli M, Guerrini R. Neuroimaging in mitochondrial disorders. Essays Biochem 2018; 62:409–421.
8. Panigrahy A, Krieger MD, Gonzalez-Gomez I, et al. Quantitative short echo time 1H-MR spectroscopy of untreated pediatric brain tumors: preoperative diagnosis and characterization. AJNR Am J Neuroradiol 2006; 27:560–572.
9. Ho ML, Campeau NG, Ngo TD, et al. Pediatric brain MRI, Part 2: advanced techniques. Pediatr Radiol 2017; 47:544–555.
10. Bray MD, Mullins ME. Metabolic white matter diseases and the utility of MR spectroscopy. Radiol Clin North Am 2014; 52:403–411.
11. Kreis R, Ernst T, Ross BD. Development of the human brain: *in vivo* quantification of metabolite and water content with proton magnetic resonance spectroscopy. Magn Reson Med 1993; 30:424–437.
12. Tochitani S. Functions of maternally-derived taurine in fetal and neonatal brain development, In: Lee DH Schaffer SW Park E, Kim HW eds. Taurine 10. Dordrecht:Springer, 2017; 17–25.
13. Tomiyasu M, Aida N, Endo M, et al. Neonatal brain metabolite concentrations: an *in vivo* magnetic resonance spectroscopy study with a clinical MR system at 3 Tesla. PLoS One 2013; 8:e82746.
14. Tomiyasu M, Aida N, Shibasaki J, et al. Normal lactate concentration range in the neonatal brain. Magn Reson Imaging 2016; 34:1269–1273.
15. Volpe JJ. Neonatal encephalopathy: an inadequate term for hypoxic-ischemic encephalopathy. Ann Neurol 2012; 72:156–166.
16. Executive summary: Neonatal encephalopathy and neurologic outcome, second edition. Report of the American College of Obstetricians and Gynecologists' Task Force on Neonatal Encephalopathy. Obstet Gynecol 2014; 123:896–901.
17. Jacobs SE, Berg M, Hunt R, et al. Cooling for newborns with hypoxic ischaemic encephalopathy. Cochrane Database Syst Rev 2013; 2013:CD003311.
18. Laptook AR, Shankaran S, Tyson JE, et al. Eunice Kennedy Shriver national institute of child health and human development neonatal research network. Effect of therapeutic hypothermia initiated after 6 hrs of age on death or disability among newborns with hypoxic-ischemic encephalopathy: a randomized clinical trial. JAMA 2017; 318:1550–1560.
19. Schwartz ES, Barkovich AJ. Brain and spine injuries in infancy and childhood, In: Barkovich AJ, Rayboud C eds. Pediatric neuroimaging, 6th ed. Philadelphia:Wolters Kluwer, 2019; 263–404.
20. Aida N, Nishimura G, Hachiya Y, et al. MR imaging of perinatal brain damage: comparison of clinical outcome with initial and follow-up MR findings. AJNR Am J Neuroradiol 1998; 19:1909–1921.
21. Rutherford M, Counsell S, Allsop J, et al. Diffusion-weighted magnetic resonance imaging in term perinatal brain injury: a comparison with site of lesion and time from birth. Pediatrics 2004; 114:1004–1014.
22. Alderliesten T, de Vries LS, Staats L, et al. MRI and spectroscopy in (near) term neonates with perinatal asphyxia and therapeutic hypothermia. Arch Dis Child Fetal Neonatal Ed 2017; 102:F147–F152.
23. Boichot C, Walker PM, Durand C, et al. Term neonate prognoses after perinatal asphyxia: contributions of MR imaging, MR spectroscopy, relaxation times, and apparent diffusion coefficients. Radiology 2006; 239:839–848.
24. Okabe T, Aida N, Niwa T, et al. Early magnetic resonance detection of cortical necrosis and acute network injury associated with neonatal and infantile cerebral infarction. Pediatr Radiol 2014; 44:597–604.
25. Cheong JL, Cady EB, Penrice J, et al. Proton MR spectroscopy in neonates with perinatal cerebral hypoxic-ischemic injury: metabolite peak-area ratios, relaxation times, and absolute concentrations. AJNR Am J Neuroradiol 2006; 27:1546–1554.
26. Bednarek N, Mathur A, Inder T, et al. Impact of therapeutic hypothermia on MRI diffusion changes in neonatal encephalopathy. Neurology 2012; 78:1420–1427.
27. Winter JD, Lee DS, Hung RM, et al. Apparent diffusion coefficient pseudonormalization time in neonatal hypoxic-ischemic encephalopathy. Pediatr Neurol 2007; 37:255–262.
28. Thayyil S, Chandrasekaran M, Taylor A, et al. Cerebral magnetic resonance biomarkers in neonatal encephalopathy: a meta-analysis. Pediatrics 2010; 125:e382–395.
29. Shibasaki J, Aida N, Morisaki N, et al. Changes in brain metabolite concentrations after neonatal hypoxic-ischemic encephalopathy. Radiology 2018; 288:840–848.
30. Lally PJ, Montaldo P, Oliveira V, et al. MARBLE consortium. Magnetic resonance spectroscopy assessment of brain injury after moderate hypothermia in neonatal encephalopathy: a prospective multicentre cohort study. Lancet Neurol 2019; 18:35–45.
31. Poretti A, Blaser SI, Lequin MH, et al. Neonatal neuroimaging findings in inborn errors of metabolism. J Magn Reson Imaging 2013; 37:294–312.
32. Schneider JF. MR spectroscopy in children: protocols and pitfalls in non-tumorous brain pathology. Pediatr Radiol 2016; 46:963–982.
33. Morton DH, Strauss KA, Robinson DL, et al. Diagnosis and treatment of maple syrup disease: a study of 36 patients. Pediatrics 2002; 109:999–1008.
34. Naughten ER, Jenkins J, Francis DE, et al. Outcome of maple syrup urine disease. Arch Dis Child 1982; 57:918–921.
35. Jan W, Zimmerman RA, Wang ZJ, et al. MR diffusion imaging and MR spectroscopy of maple syrup urine disease during acute metabolic decompensation. Neuroradiology 2003; 45:393–399.

36. Heindel W, Kugel H, Wendel U, et al. Proton magnetic resonance spectroscopy reflects metabolic decompensation in maple syrup urine disease. Pediatr Radiol 1995; 25:296–299.
37. Sato T, Muroya K, Hanakawa J, et al. Neonatal case of classic maple syrup urine disease: usefulness of (1) H-MRS in early diagnosis. Pediatr Int 2014; 56:112–115.
38. Hamosh A, Johnston MV. Nonketotic hyperglycinemia. In: Scriver C, Beaudet A, Valle D, et al. eds. The metabolic and molecular bases of inherited disease, 8th ed. New York: McGraw-Hill, 2001; 2065–2068.
39. Shah DK, Tingay DG, Fink AM, et al. Magnetic resonance imaging in neonatal nonketotic hyperglycinemia. Pediatr Neurol 2005; 33:50–52.
40. Tomiyasu M, Shibasaki J, Kawai Y, et al. Quantification of brain glycine in an infant with nonketotic hyperglycemia: a serial proton magnetic resonance spectroscopy study. Proceedings of the 28th annual meeting of ISMRM 2020, Paris, 2020; 4678.
41. Barkovich AJ, Patay Z. Metabolic, toxic, and autoimmune/inflammatory brain disorders, In: Barkovich AJ Rayboud C eds. Pediatric neuroimaging, 6th ed. Philadelphia:Wolters Kluwer, 2019; 81–262.
42. Trinh BC, Melhem ER, Barker PB. Multi-slice proton MR spectroscopy and diffusion-weighted imaging in methylmalonic acidemia: report of two cases and review of the literature. AJNR Am J Neuroradiol 2001; 22:831–833.
43. Aida N, Tomiyasu M, Hanakawa J, et al. MRI and MRS findings in neonates with methylmalonic acidemia. Proceedings of the 46th annual meeting of JSNR, Tokyo, 2017; 77.
44. Takanashi J, Barkovich AJ, Cheng SF, et al. Brain MR imaging in neonatal hyperammonemic encephalopathy resulting from proximal urea cycle disorders. AJNR Am J Neuroradiol 2003; 24:1184–1187.
45. Gropman A. Brain imaging in urea cycle disorders. Mol Genet Metab 2010; 100 (Suppl 1):S20–30.
46. Saneto RP, Friedman SD, Shaw DW. Neuroimaging of mitochondrial disease. Mitochondrion 2008; 8:396–413.
47. Farina L, Chiapparini L, Uziel G, et al. MR findings in Leigh syndrome with COX deficiency and SURF-1 mutations. AJNR Am J Neuroradiol 2002; 23:1095–1100.
48. Mitani T, Aida N, Tomiyasu M, et al. Transient ischemic attack-like episodes without stroke-like lesions in MELAS. Pediatr Radiol 2013; 43:1400–1403.
49. Aida N. MELAS (Mitochondrial myopathy, encephalopathy, lactic acidosis, and stroke-like episodes), In: Aoki S, Aida N, Ida M, Oba H, eds. Well-understandable brain MRI, 4th ed. Tokyo:Gakken Medical Shujunsha, 2020; 452–453. (in Japanese)
50. Koenig MK, Hodgeman R, Riviello JJ, et al. Phenotype of GABA-transaminase deficiency. Neurology 2017; 88:1919–1924.
51. Tsuji M, Aida N, Obata T, et al. A new case of GABA transaminase deficiency facilitated by proton MR spectroscopy. J Inherit Metab Dis 2010; 33:85–90.
52. Ichikawa K, Tsuji M, Tsuyusaki Y, et al. Serial magnetic resonance imaging and ^{1}H-Magnetic resonance spectroscopy in GABA transaminase deficiency: a case report. JIMD Rep. 2019; 43:7–12.
53. Provencher SW. Estimation of metabolite concentrations from localized *in vivo* proton NMR spectra. Magn Reson Med 1993; 30:672–679.
54. Tachibana Y, Aida N, Enomoto K, et al. A case of Sjögren-Larsson syndrome with minimal MR imaging findings facilitated by proton spectroscopy. Pediatr Radiol 2012; 42:380–382.
55. Osaka H, Takagi A, Tsuyusaki Y, et al. Contiguous deletion of SLC6A8 and BAP31 in a patient with severe dystonia and sensorineural deafness. Mol Genet Metab 2012; 106:43–47.
56. Mano T, Ono J, Kaminaga T, et al. Proton MR spectroscopy of Sjögren-Larsson's syndrome. AJNR Am J Neuroradiol 1999; 20:1671–1673.
57. Willemsen MA, Van Der Graaf M, Van Der Knaap MS, et al. MR imaging and proton MR spectroscopic studies in Sjögren-Larsson syndrome: characterization of the leukoencephalopathy. AJNR Am J Neuroradiol 2004; 25:649–657.
58. Adam MP, Ardinger HH, Pagon RA, et al. editors. GeneReviews®. Seattle: Universityof Washington, 1993-2021. https://www.ncbi.nlm.nih.gov/books/NBK1116/. (Accessed: March 22, 2021)
59. Aida N, Tomiyasu M, Enokizono M, et al. MRI/MRS findings of cerebral creatine deficiencies. Proceedings of the 43rd annual meeting of JSMRM, Tokyo, 2015; 173.
60. Clark AJ, Rosenberg EH, Almeida LS, et al. X-linked creatine transporter (SLC6A8) mutations in about 1% of males with mental retardation of unknown etiology. Hum Genet 2006; 119:604–610.
61. Rosenberg EH, Almeida LS, Kleefstra T, et al. High prevalence of SLC6A8 deficiency in X-linked mental retardation. Am J Hum Genet 2004; 75:97–105.
62. Newmeyer A, deGrauw T, Clark J, et al. Screening of male patients with autism spectrum disorder for creatine transporter deficiency. Neuropediatrics 2007; 38:310–312.
63. Wada T. Summary in clinical research of cerebral creatine deficiency syndromes supported by Japan Ministry of health, labor and welfare scientific research grant 2015. https://research-er.jp/projects/view/918118. (Accessed: March 22, 2021)
64. Bianchi MC, Tosetti M, Battini R, et al. Treatment monitoring of brain creatine deficiency syndromes: a ^{1}H- and ^{31}P-MR spectroscopy study. AJNR Am J Neuroradiol 2007; 28:548–554.
65. Kurosawa Y, Degrauw TJ, Lindquist DM, et al. Cyclocreatine treatment improves cognition in mice with creatine transporter deficiency. J Clin Invest 2012; 122:2837–2846.
66. Akiyama T, Osaka H, Shimbo H, et al. A Japanese adult case of guanidinoacetate methyltransferase deficiency. JIMD Rep 2014; 12:65–69.
67. Steinfeld R, Grapp M, Kraetzner R, et al. Folate receptor alpha defect causes cerebral folate transport deficiency: a treatable neurodegenerative disorder associated with disturbed myelin metabolism. Am J Hum Genet 2009; 85:354–363.